The microscopic theory of superfluid ^{4}He

J. X. Zheng-Johansson[1*], B. Johansson[2], and P-I. Johansson[3]

1. H. H. Wills Physics Laboratory, Bristol University, Tyndall Avenue, Bristol, BS8 1TL, England
2. Condensed Matter Theory Group, Department of Physics, Uppsala University, Box 530, 75121
Uppsala, Sweden
3. Department of Neutron Research, Uppsala University, Studsvik 611 82, Sweden

(October, 2002)

We present a microscopic theory of superfluid ^{4}He, formulated using the overall experimental observations as input information. With the theory of a consistent basis, we answer all of the essential questions regarding He II. To conform to the overall key experimental observations, we show that in their coexistence at a higher T the superfluid and normal fluid atoms necessarily aggregate in separate large regions, which with falling T reduces to predominantly superfluid aggregates. In a superfluid aggregate, termed a **momenton**, the helium atomic wave-packets primarily perform **localized (harmonic) oscillations** about sites fixed on the momenton, facilitating excitation states of discrete energy levels. The predominant thermal excitation in the superfluid equilibrium is hence between these discrete levels, i.e. in the form of single phonons. Superposed to the coherent oscillations of the single atoms above, the **momenton waves**, comprising the *in phase, simultaneous* oscillations of all of the atoms in each momenton, give rise to the so-called second sound wave, which contribution to the total excitation and energy is however negligible. The superfluid atoms are strongly correlated, due to a many-quantum-atom correlation, having a binding energy -7.2 °K/atom as from experiments; from this we suitably define a **superfluid bond**, $\Delta_b \simeq 7.2$ °K/atom. Δ_b is substantial, on the scale of total excitation energy (~ 15 °K) or of the binding energy of He I (~ 3 °K/atom), and inevitably dominates the phase stability of He II. Accordingly in the superfluid in *quasi equilibrium* between 0.6-2.17 °K, thermal excitation is predominantly due to the break-up of Δ_b, at an activation energy $\Delta_b + \delta_v \simeq 8.6$ °K. This yields the experimentally observed λ specific heat, and in turn the **inelastic damped-Bragg scattering** of neutrons at 1.93 Å^{-1}. By embodying these concepts pertaining to static structure of the fluid, atomic bobnding and atomic dynamics, we establish equations of motion for the superfluid atoms, both semi-classical and quantum mechanical, in a coordinate decomposition scheme. Based on their solutions, and the results from a corresponding statistical thermodynamic treatment, we have been able to quantitatively predict all the essential properties of He II, including the full excitation spectrum (dividing in $q < 1.93 - \sigma/2$, $1.93 - \sigma/2 < 1.93$ and $q = 1.93$ Å^{-1}), the two fluid fractions, the specific heat (dividing in the T^3- and the λ-C_V regions), the superfluid phase transition temperature T_λ, and in a separate paper II the critical velocity v_c, the total number of excitation states and the superfluid viscosity; all of which are in good overall good agreements with experiments. We have also evaluated the zero point energy, the potential energy, the first order thermodynamic functions including $U(T)$, $A(T)$, $S(T)$ and $J(T)$ of which $S(T)$ can be satisfactorily compared with experimental data; we also formally present the continuity and stability conditions of the superfluid, and the dynamics structure factor due to the Δ_b excitation. The microscopic scheme also facilitates a novel, consistent **QCE superfluidity mechanism**, presented in paper II. Also on the basis of the scheme, we show that the circulation qunataization is due to a **circular atomic wave self-interference**. As a whole, in terms of the theory proposed in this work not only are all the explanations regarding the essential properties of He II of a consistent theoretical grounding, but also are consistent with the concep-

*Email: jxzj@mailaps.org

tions that apply to common condensed matter systems and with the common laws of physics. The series of novel concepts evolving from this work can give significant impact also to the understanding of other superfluids.

I. INTRODUCTION

Liquid ^{4}He exhibits properties which are altogether anomalous at temperatures below 2.17 K, i.e. in the superfluid phase, He II. The two most striking ones are its restraint from solidification down to zero K under ambient pressure[1] and its superfluidity.[2−4,6,5,7,8] Some of the anomalies, such as the large zero point energy[9] and the volume expansion with falling T,[10] can be traced immediately to the extreme chemical character of the ^{4}He atom, which being light, small and inert. Many others, on the other hand, cannot be understood in this simple manner; the far-most of these are the superfluidity, the circulation quantization,[11−13] the λ specific heat about the phase transition,[14] the anomalous excitation spectrum,[15] and the anomalous thermal conductance[16] and melting curve.[17] These properties can be seen to be largely dictated by the collective and correlation behaviour of the atoms in the condensed form and, their interpretations inevitably require firstly an adequate microscopic depiction of this condensed system. Since the discovery of the superfluidity of He II during 1911,[10] - 1938[3,4,8] extensive investigations have been made on this system both experimentally and theoretically; although, experimentally direct probe of the excitations using neutron scattering technique, which informs a great deal about the microscopic dynamics, did not begin until the end of 1950's.[15] Many comprehensive reviews on this subject haven been given.[18−33]

Theoretically, the current understanding of He II is essentially based on the compilation of a few distinct models proposed by London,[34] Landau,[35] and Feynman[36] during 1938-1950's; a number of other studies[37−42] have also historically contributed to the now accepted "single" model. With one thing in common, all these models assume that He II consists of two coexisting fluids, the normal fluid and the superfluid, and the two fluids interpenetrate on an atomic scale. The otherwise main concerns in each of the models have been the excitation scheme of the superfluid and a (corresponding) superfluidity mechanism. London[34,18] suggested that of the tow fluids, the superfluid undergoes Bose-Einstein condensation (BEC), i.e. it consists of atoms that condense in the momentum space into a single degenerate state and in real space are motionless and non-interacting. Accordingly, the BEC implies a non-viscous and zero-entropy superfluid, and hence yields the superfluidity. This is despite the fact that, in his early view, London also foresaw the possibility that the quantum states of liquid He II would partly have the feature of the vibration states (phonons) of Debye in the theory of metals[43]. As opposed to London, Landau[35] described He II as having two elementary excitations, phonons created mainly at a low T, and rotons at a higher T. Superfluidity will result if the velocity of a flow motion is lower than that of the particles from the elementary excitations. A landmark success of Landau's model is the excitation spectrum he phenomenologically designated in order to achieve a desirable (lambda) specific heat; the key feature of the spectrum has been remarkably corroborated, firstly by the neutron scattering experiment of Larsson et al. in 1958.[15] However, Landau did not provide a microscopic scheme as to how the two elementary excitations occur, and in particular, what actually a "roton" is. Furthermore, for the superfluidity Landau predicted a critical velocity which is at least two orders of magnitude too large than the experimental values, and contains no mechanism for channel width dependence. The two distinct models above were linked together by Bogoliubov[38] who suggested that the majority of superfluid is in BEC state in which, in contrast to London's BEC, the atoms interact weakly, and that the transition of the atoms from the BEC state to the quasi particle state produces the two types of elementary excitations of Landau. These two or three models are essentially phenomenological. Feynman[36] in the 1950's, in a semi-microscopic description, suggsted the excitations (of both types) result from the superfluid, being the ground state, to the normal

fluid. Quantitatively based on variational principle for some trial wavefunction, where the microscopic picture for atomic motion and excitation is however essentially lost, he gave an improved prediction of the excitation spectrum (1954; Feynman and Cohen,1956). At a microscopic scale, Feynman briefly, qualitatively described the atoms as being confined in the cages built by neighboring atoms (– a picture held also in the present work), but primarily showed the "rotons" of Landau, representing the higher energy excitations, to be possible from a symmetry point of view. Taking Landau's critical velocity as a valid start, but to rescue it from the clearly large quantitative discrepancy, Feynman (1955) assumed there present even lower excitations, vortices; the creation of maximum vortices yields critical velocities giving the right magnitudes. Until 1990's, the widely adopted (excitation) model of He II is the up-dated compilation of the models by the four individuals, referred to below as the LLBF theory, is as follows:[44] the superfluid corresponds to a BE condensate, which becomes hundred percent at zero °K; the two elementary excitations result from the shuttling of atoms between the superfluid - the BE condensate – and the normal fluid. Whilst the LLBF model assumes that, at zero °K, the BEC, being identified with the superfluid, is hundred percent, recent experiments have shown the BEC is only $9 \sim 10$ percent. This conflict was circumvented by Glyde and Griffin in the 90's,[42] in proposing that the BEC fraction as well as the helium atom mass is modified due to an interaction of the superfluid with the normal fluid atoms. This apparent improvement does not however remove the basic difficulties pertaining to the foundation of the LLBF model. Theoretical studies of liquid ^{4}He in the past two decades have otherwise largely involved quantum simulations including variational MC[47−50] and path integral MC,[51,52] which essentially pertain to a more accurate representation of Feynman's (or, the LLBF) excitation model. More broadly, these studies are not yet apt to yield the microscopic information of the superfluid atoms, regarding configuration, motion and dynamics, and are even far remote from touching the microscopic scheme of superfluidity, and circulation quantization. The Green's function technique for treating many-body problems is not feasible today for treating such complex system as He II, in respect of its above ground propety in parcticular.[33,54]

As a whole, the LLBF theory encounters various difficulties which give rise to a variety of self-contradictions, and therefore does not represent an ultimately satisfactory theorization for the superfluid He II. Its most significant difficulties may be outlined as follows (further discussions are pointed to each relevant sections). 1). The LLBF thermal excitation picture (when faithfully formally represented) inevitably predicts a broad peak in the dynamics structure factor, in direct contradiction to experimental observations (Sec. II A). 2). The *non-viscous, non-interacting* superfluid atoms, which although is sensibly not held in the dynamic model of the LLBF theory but is nevertheless a base for the LLBF explanation of superfluidity – see item 4) below, directly contradicts with the fact that superfluid atoms are strongly correlated and the actually substantial atomic binding energy (Sec. II B). 3). A mixture of two fluids *interpenetrating on an atomic scale* lacks the mechanism for the maintenance of the atomic bonding characters of the respective fluids (Sec. II B). 4). The critical velocity criteria for superfluidity of Landau[35] and Feynman[36] (1955) have both incorrectly ignored the primary low energy excitations due to phonons (which in fact sensibly presents in the LLBF superfluid dynamic picture), and the comparison of velocities of different masses they made does not conserve energy (Ref. 55).[45]. 5). The "roton" picture does not predict the experimentally observed overall features in the excitation at q_b (Sec. II B). 6). The "Bose-Einstein condensation" picture is itself not capable of explaining superfluidity.[56] These difficulties inherent in the foundation(s) of the LLBF theory, cannot to us just be removed by a few minor improvements. Therefore, as the motivation for beginning this work, we felt it necessary to develop a theory that starts from an alternative – an essentially consistent – theoretical grounding.

To provide an overall satisfactory interpretation of the complex behavior of He II, we first, in Secs. II-III, carry out a systematic derivation of a (microscopic) theory by using, to the broadest possible extent, the key experimental properties of liquid ^{4}He as input information. Three key questions are to be addressed: 1) do the superfluid atoms primarily perform *localized oscillations*, or, *diffusion*, or do they *stand still* (see Sec. II A) ? 2) whether and how the atoms are interacting (see Secs. II B, III)? 3) when the two fluids coexist in He II in the higher T end, do the superfluid atoms aggregate in large regions such that they possess

a characteristic bonding energy, or, do they intermingle with the normal fluid on an atomic scale (Sec. II C)? The answers to these questions have been achieved in this work after making iterative contrasts between what is predicted by an assumed "theoretical model" and what is observed by experiment, and between the prediction of one property and its implications for others. The key components of the theory are therefore already characterized in Secs. II-III. In Secs. IV - VIII we establish the corresponding formal theoretical and quantitative description of He II, including the composition structure of He II (Sec. IV), the set-up of equations of motion of the superfluid atoms (Sec. V) and solving (V B-V C), and the prediction from the solution of the physical properties, including excitation spectrum (V B,V C), the stability condition of the superfluid (Sec. VI), the quantization of circulation (Sec. VII), and the scattering function near the superfluid bond excitation (Sec. VIII). The superfluidity (its mechanism and the critical velocity) is treated in a separate paper, II.[55] These above contents constitute the microscopic part of the theory of superfluid ^{4}He. Sections IX-X present a corresponding statistical thermodynamics description of He II. Brief description of the theory has previously been presented in unpublished internal reports[57] except for Ref. 57 (2000) which mainly discusses the experimental probe of the QCE effect as fully presented in paper II.

II. THE FORMULATION OF THE MICROSCOPIC THEORY BASED ON OVERALL EXPERIMENTAL OBSERVATIONS

The static structure factor, $S(q)$, of the (pure) superfluid, as has been probed both by neutrons[58,59] and by X-ray,[60−63] exhibits a heavily damped first peak at about $q_b \approx 1.93$ Å^{-1} and almost vanishing higher rank peaks (FIG. 1b). Immediately, this signatures that the superfluid retains only a short range ordering, with a mean atomic separation $a = 2\pi/q_b = 3.3$ Å. The detail of this ordering is not our concern; for a large part of our purpose here it suffices to conveniently, fully represent the atomic configuration with three orthogonal arrays of atomic chains in X, Y, Z directions, we thus have a simple cubic *pseudo lattice* with a lattice constant a and a *pseudo lattice* reciprocal lattice vector $b = 2\pi/a = q_b$; see further Sec. V B.

Experiments, including specific heat (Secs. I,II), frequency dispersion (Sec. I), and second sound,[64−66] have commonly shown that He II is an coexistent of the superfluid between about 2.17 to 0.6 ($\sim$1) °K, reduces to predominately a (pure) superfluid below 0.6 °K, and at zero °K is hundred percent a superfluid. Below in Secs. II A-II C we infer from experiments the excitation and dynamic schemes in the two respective temperature regions, and the microscopic composition structure of the two-fluid coexistent and the related dynamics.

A. Thermal excitation via single phonons and atomic dynamics scheme of the superfluid equilibrium

(i) The dynamic structure factor The most revealing indication as to the underlying dynamic scheme in the superfluid equilibrium, which predominates below $\lesssim 0.6$ °K, is from the dynamic structure factor $S(q, \omega)$. The measurements from inelastic neutron scattering[15,67−73] have shown that the $S(q, \omega)$ of He II is characteristically different at T below and above T_λ, at a given momentum transfer q, with q raging from 0 up to at least 2.4 Å^{-1}.[74] The strongest distinction presents at an intermediate q (~ 1.1 Å^{-1}).[68−70] Here, the $S(q, \omega)$ exhibits a superposition of a sharp and a broad peak on the ω axis, ω being the neutron energy transfer.[68] The broad peak, which has a non-vanishing intensity at $\omega = 0$, at T above T_λ identifies with the broad diffuse peak of the normal fluid He I and reduces smoothly in intensity as T is reduced to below T_λ. The sharp peak appears abruptly as T falls just below T_λ; its intensity increases as T falls and then basically stabilizes from about 1 °K downwards.
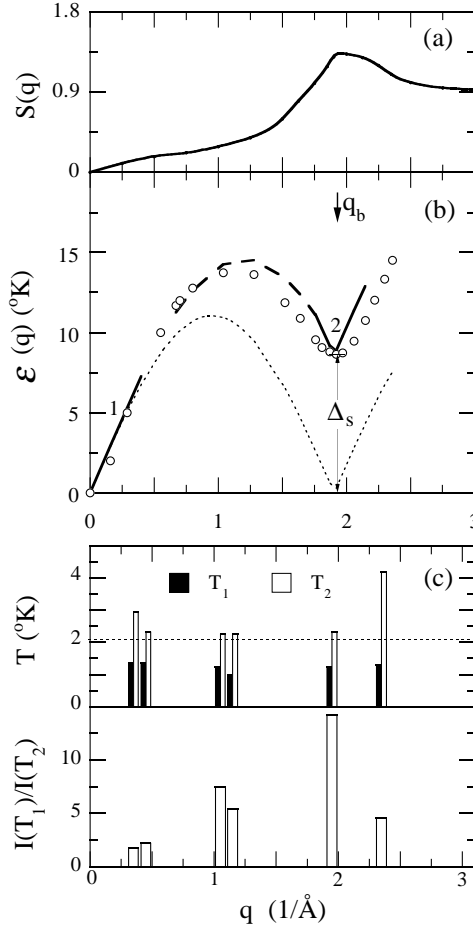
FIG. 1. (a). The experimental static structure factor $S(q)$ 60 is plotted to assist discussions in the text. (b). Total thermal excitation energy $\varepsilon(q)$ versus the neutron momentum transfer q (equal to phonon wave number K) for the superfluid of He II. Circles indicate data points from inelastic neutron scattering measurement at 1.12 °K67. The solid and dashed curves show the theoretical dispersion (Sec. V); see further FIG. 7. The dotted curve illustrates a regular (i.e. with no superfluid bond excitation and with no nearest-neighbour repulsion) longitudinal single phonon energy dispersion, given by Eq. (26a) for all K values, obtained with $a = 3.3$ Å $(2\pi/a = 1.93$ Å$^{-1})$. (c). Lower graph: ratio of neutron scattering intensities, $I_1(T_1)$ and $I_2(T_2)$, at two temperatures T_1 $(< T_\lambda)$ and T_2 $(> T_\lambda)$ as indicated in the upper graph.

It is natural to correlate this T dependence of the scattering intensity with the two-fluid fraction variation just mentioned. Woods and Svensson[68] based on quantitative evaluation, have shown that indeed the sharp and the broad peaks are attributable to the superfluid and the normal fluid respectively. Now, for the superfluid of concern, we can thus concentrate oursevels below only on the sharp peak. The compelling feature with the sharp peak is that, with the observed finite width being in principle only due to the finite instrumental resolution,[25,68,69,75] it has the three characteristics of the phonon excitations in a crystalline solid: it is qualitatively narrower, it has a high frequency cut-off and, it peaks at a finite ω and has a vanishing intensity at zero ω. Such a sharp peak in $S(q, \omega)$ which represents the probability that an energy transfer of ω occurs inevitably implies that, the excitation must have occurred between two discrete energy levels. Experiments using pulse transmission techniques[76] have on the other hand shown that, at long wavelengths, the excitations are via sound waves. The combined information above hence characterizes the excitation to be via the creation and annihilation of phonons, each having an energy quantum, $\mathcal{E}(q)$. We refer to these as "single phonons" to separate from the "collective phonons" of Sec. II B. It should be remarked that, phonon excitation, with a well defined atomic dynamic scheme

5

in Debye's theory of solids (1912),[43] is terminological also held in the LLBF theory for He II but, as will be illustrated in FIG. 2 below, it clearly is unable to be produced by the dynamics scheme of the LLBF theory.

To infer from the above feature of excitation the underlying atomic dynamic scheme, we shall first be guided by a general principle of quantum mechanics, which states that the state of a quantum particle will be discretized when under spatial confinement. In a bulk superfluid – a condensed atomic assembly, if and only if assuming the atoms are localized – in both ends of its excitation, then each atom is wholly confined by its surrounding atoms, as is in a solid. And only then, the atom will then acquire fully discretized states; the transition between these states will result in the sharp peak of the $S(q,\omega)$, as is how such a sharp $S(q,\omega)$ peak in a crystalline solid (at low T) regularly results. (Although, the two present a few important distinctions which we discuss in Sec. V B.) Based on the above arguments and furthermore on the variety of other uniform indications to be described below, we propose:

> In the superfluid equilibrium, the thermal excitation is predominantly via the creation and annihilation of (longitudinal) single phonons, whcih predominate at temperatures below 0.6 (~ 1) $^\circ$K. This excitation can only have occurred within the (pure) superfluid and resulted from **localized (harmonic) atomic oscillations** (of an amplitude $\mathbf{u}(\mathbf{R})$), referred to as the LAO dynamics scheme. Each oscillator roughly corresponds to a single helium atom, separated by the interatomic spacing of He II, $a \simeq 3.3$ Å, and oscillates in a potential well V (of a depth of ~ -7.2 $^\circ$K/atom as will be detailed in Sec. II C).

Based on the LAO dynamics scheme, the solution of equations of motion of the superfluid atoms in Sec. V actually reproduces the experimentally observed excitation feature, i.e. the excitation is between discretized energy levels ϵ_n, $n = 0, 1, \ldots$ (FIG. 2a), each differing by an energy quantum of a phonon, $\mathcal{E}(K)$. In effect, LAO is the only dynamic scheme able to give rise to a sharp diffraction peak for the superfluid. In contrast, the LLBF picture of phonon excitation (FIG. 2b), namely *the excitation results from the knocking out of atoms from the Bose-Einstein condensate into the normal fluid*, will incorrectly predict a broad peak of the dynamic structure factor. Evidently, this is because the energy of an atom in the normal fluid end, $E(p)$ at a given momentum p, and consequently the excitation energy $E(p) - E_{BEC}$, are continuous, despite the single valued BEC energy E_{BEC}.
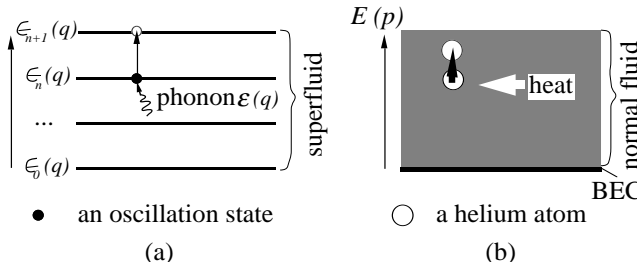

FIG. 2. Excitation scheme for the superfluid equilibrium as proposed: (a) by the present theory. The excitation is via the creation of a single phonon, corresponding to a transition between the discrete energy levels $\epsilon_n(q)$ and $\epsilon_{n+1}(q)$ of the oscillation mode q of the localized (relative to ξ) superfluid atoms. (b) by the LLBF theory. The excitation of the helium atomic motion is produced by a transition from the single degenerate state of the "Bose-Einstein condensate" (the superfluid) of energy E_{BEC}, to the continuous normal-fluid energy $E(p)$ at a given momentum p.

The inference of localization and the LAO from the sharp $S(q,\omega)$ peak is further supported by the observation of a one-to-one link between a sharp $S(q,\omega)$ (or broad) peak and atomic localization (or diffusion) which being general and system-independent, as has been identified, for the first instance, by Sköld and Larsson[77] in their comparison of the scattering features from the solid and the classical liquid phase of argon, and similarly from the two different phases of other systems. Where, the broad scattering intensity at lower energies

was assigned to be due to diffusion, the so called "quasielastic scattering". In another example, a sharp $S(q,\omega)$ peak centered at a finite ω for a fixed (intermediate) q has also been observed in various metallic liquids, such as lead by Egelstaff[78] and rubidium by Copley et al.[79] Copley and Lovesey[80] correlated that feature to the stronger metallic bonding of Rb compared to that of a classical liquid. We can readily infer that the strong bonding functions to confine – to localize – the atomic motion.

The LAO scheme also immediately explains as to why mainly the intermediate q scattering rather than the low q is specific with the superfluid; at a $q < 0.4$ Å^{-1}, for T below and above T_λ, the position, intensity and width of the $S(q,\omega)$ peak of liquid helium exhibit no distinct changes except that the rate of increase of the width is slowed down.[70] Since $K (\equiv q) \sim 1.1$ Å^{-1} corresponds to a wavelength $\lambda (= 2\pi/q) \sim 10$ Å crossing over only a few atomic spacings (with $a \simeq 3.3$ Å). Hence a coherent oscillation, if to occur at such a short wavelength, would require all of the atoms move cooperatively and the atoms must therefore be localized. By contrast, at long wavelength crossing over many atoms, the oscillation occurring by means of density fluctuation is insensitive to diffusion of some individual atoms. Indeed, in addition to the observation for liquid helium above, neutron scattering experiments have shown that the $S(q,\omega)$ functions from normal liquids all present a certain sharp peak at $q \underset{\sim}{<} 0.4$ Å^{-1}.[80]

(ii). The excitation spectrum The LAO scheme is further pointed to by the excitation spectrum (FIG. 1b), $\omega(q)$ due to the sharp peak of $S(q,\omega)$[67] in two respects. First, except for the peculiar non-zero value, $\Delta_s \simeq 8.6$ °K at $q_b \simeq 1.93$ Å^{-1}, $\omega(q)$ has a sinusoidal dispersion which is the solution of the equation of motion of (relatively) localized helium atoms, Eq. 26 in Sec. V B, for the longitudinal mode. Second, the solution informs the linear sector to be due to propagating elastic sound waves, here phonon waves, of a velocity 238.9 m/sec which is in near exact agreement with the first sound velocity $c_1 = 239$ m/sec from pulse transmission experiments.[76] Moreover, the experiment by Woods showed that the slope here is independent on T,[81] and disproves the postulation[82] that the slope might be instead due to the two-fluid density variation with T $(c_1(\rho_s/\rho)^{1/2})$. Furthermore, the dispersion "period", $q_b = 2\pi/a \simeq 1.93$ Å^{-1}, giving $a \simeq 3.3$ informs the oscillator size $a_\rho \sim 3.6$ Å,[83] which is just a helium atom. This can be similarly seen from the upper limit, $q \simeq 0.6$ Å^{-1}, of the propagating phonon wave which development would require at least be a few oscillators within a wavelength. In contrast, the part of the "in-phase" oscillation of a large (N_M) number of superfluid atoms (to be discussed in the next section), which alone is similar to the weekly interacting BEC wave or the zero sound wave[40] in the LLBF terminology, has a maximum dispersion period $K_M \propto 2\pi/N_M a << q_b$ and an excitation energy negligibly low compared to the one of the single phonon here.

(iii). The T^3 specific heat The LAO scheme is indicated by the Debye T^3 behavior of the specific heat C_V of He II between $0 \sim 0.6$ °K (FIG. 3a).[84] Insofar as a non-conducting condensed atomic system is in question, a Debye T^3- C_V is broadly known to be necessarily given rise to by an atomic assembly where the atoms are localized and perform harmonic oscillations; the superfluid is not an exception as Sec. IX D explicitly treats based on statistical thermodynamics. By contrast, a classical fluid consisting of diffusive atoms generally shows a Petit-Dulong heat capacity. It follows that, the LLBF excitation scheme will inevitably yield a specific heat strongly bearing the feature of the normal fluid, which cannot be of a T^3 behavior. Furthermore, the theoretical Debye $C_V(T)$ obtained in Sec. IX D, when fitted to the experimental C_V data, produces a longitudinal phonon velocity of 241 m/sec. This value agrees (within experimental error) with the c_1 value (239 m/sec) from pulse transmission[76] as well as phonon velocity (238.9 m/sec) from the excitation spectrum discussed in (ii).
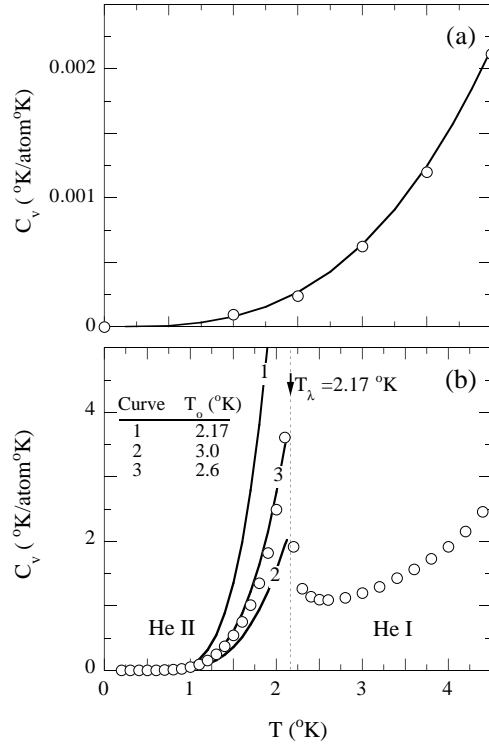
FIG. 3. Specific heat of He II, $C_V(T)$. Circles represent experimental values (Refs. **??**); solid lines are statistic thermodynamic results of Sec. IX as based on the present microscopic theory of Secs. II-V. (a) for T below 0.6 °K, the theoretical $C_V(T) \propto T^3$, Eq. $(74)'$, is given by the derivative of the internal energy obtained from a canonical ensemble average over the states, with a Debye type of density of states, of the independent, indistinguishable single phonons, which are produced due to in real space the harmonic oscillations in the normal coordinates of the (N) independent, localized superfluid atoms relative to ξ. (b) from 0.6 to just below 2.17 °K, the theoretical λ-$C_V(T)$ (Eq. $(74)'$) results principally from the conversion of the superfluid to the normal fluid, via the excitations of superfluid bonds. The lower and upper limits of T_o, 2.17 and 3.0°K, yield the uncertainty boundaries of the theoretical $C_V(T)$ shown by the solid lines 1 and 2; $T_o = 2.6$ °K gives the optimum $C_V(T)$, solid line 3.

(iv). The inferred diffusion rate   The LAO scheme is directly supported by the solid-like low diffusion rate in He II, being 10^{-8} cm^2/sec as Eq. 26 in Sec. V C shows. The associated diffusion barrier implies a negative potential well in which the atom executes oscillation.

(v). The capability of predicting superfluidity   The preceding observations inform that the superfluid atoms are not *standing-still* (in either the absolute or relative coordinates), and rather, the superfluid is fully thermally excited, with the excitation states, as Sec. IX shows, exhibiting a Planck distribution. The LAO scheme and the implied property above are furthermore supported by the fact that, as paper II shows, on the basis of the LAO scheme the QCE superfluidity mechanism can consistently, quantitatively predict superfluidity and critical velocity both in satisfactory agreements with experimental data.

The one-to-one connection between an excitation spectrum as FIG. 1b for He II and a fully excited He II is an inevitable truth, if one compares it with the analogous excitation phenomena of the vast body of crystalline solids, in terms of the phonon feature in general and the Kc_1 behaviour in the linear sector in particular. Had Landau's criterion of critical velocity for He II, namely that if $v_s < c_1$ there is no phonon excitation, reflected the truth, then one will be led to the inevitably untrue conclusion, that any piece of crystalline solid moving, say against the surface of the ground, with a speed less than its sound velocity would be in superfluidity motion.

B. The superfluid bond excitation and atomic dynamics scheme; the gradual phase transition of the superfluid

The atomic localization in the LAO dynamics scheme derived in Sec II immediately suggests that, in the superfluid the atomic bonding has undergone a qualitative enhancement compared to the van der Waals (vdW) "bonding" energy of the normal fluid He I. We represent the former by **superfluid bond**, Δ_b, which is defined to be the negative of the binding energy per superfluid atom that is given rise to by the attraction from many superfluid atoms within their correlation regime, Υ. Clearly, Δ_b is directly associated with the stability of the superfluid phase. We propose:

A *quasi equilibrium* process is predominated by excitations of superfluid bond (Δ_b) in two closely related Δ_b dynamics schemes, where Δ_b represents an attractive energy barrier which prevents the reference atom 1) from diffusing into its neighbouring site within the superfluid when locally perturbed, due to thermal fluctuation or an external incidence such as a neutron, and, 2) from transforming into the normal fluid state when globally perturbed, e.g. by bulk heating-up between 0.6 ∼2.17 °K.

By the definition above, Δ_b can be expressed by

$$\Delta_b = -U_{s0} - <\epsilon_n> + \overline{u}_s. \tag{1}$$

Where, U_{s0} is the ground-state cohesive energy (per atom) of the superfluid, representing the depth of the potential well in which a He atom is confined (FIG. 4a1); $U_{s0} = -7.2$ °K/atom as given by thermal measurements at SVP.[88,18] $<\epsilon_n>$ is the per-atom kinetic energy of superfluid atoms and is $<< U_{s0}$ as will be verified in Sec. IX. $\overline{u}_s(< 0)$ represents the "long range" attraction energy by atoms in the entire fluid bulk, so an atom in $(\overline{u}_s, 0)$ can diffuse virtually freely. The superfluid atom is, as Sec. V A will show, localized with respect to a kinetic energy even up to $-U_{s0}$, thus one can expect $\overline{u}_s << \Delta_b$; hence we have

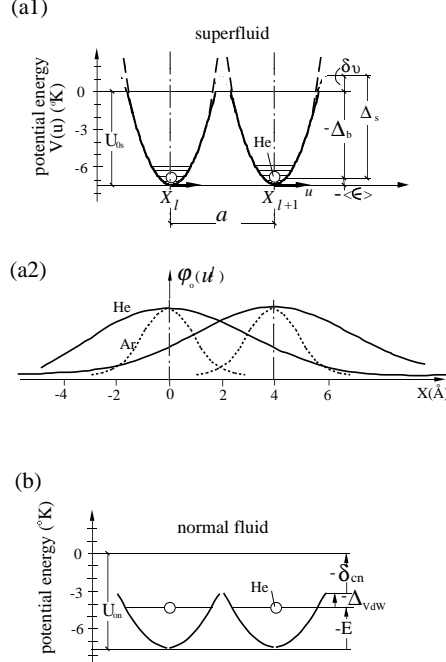$$\Delta_b \approx -U_{s0} = 7.2 \quad (°K). \tag{1}'$$

(a1)

(a2)

(b)

9

FIG. 4. (a1). The potential energy $V(u)$ for a superfluid atom at X_l and for one separated at a distance a at X_{l+1}, solid parabolic curves, theoretically constructed as in Eq. (20)" illustrated for the mode $Ka = 0.5\pi$; see FIG. 8 for $V(u)$ at different K values. In the potential wells, the superfluid atoms perform independent harmonic oscillations in the relative coordinates ξ. The potential well depth V_0 is given by the experimental ground state energy $U_{0s} = -7.2$ °K/atom 88. The activation of an atom from the bottom of the well to just above zero, at a energy cost $\Delta_s = \Delta_b + \delta_v$, represents the excitation of a superfluid bond Δ_b, with a site creation energy δ_v. $< \epsilon >$ represents the average kinetic energy per superfluid atom, and by Sec. IX $< \epsilon > << U_{0s}$, hence $\Delta_b \simeq U_{0s}$. The dashed lines indicate the repulsive part of the potential, $V(u) > 0$, and is associated with the phonon excitation within $0.6 \leq K \leq 1.4$ (1/Å) where $\mathcal{E}(K) > \Delta_b$; cf. FIG. 1. (a2) The ground state wavefunctions (solid curves) resulting from the solution of equation of motion of superfluid atoms. The dotted curves show wavefunctions for Ar atomic mass. (b). Illustration of the normal fluid potential energy for two adjacent atoms. $E = U_n - U_{on} \simeq 3.1$ °K for T just below T_λ is the kinetic energy, and Δ_{VdW} the average Van der Waals bonding energy. The diffusion barrier height between the adjacent atoms, being about 1.6 °K relative to E, is estimated such that it produces a diffusion constant in the order of 10^{-4} cm^2/sec at 1 °K, a typical value for liquids. $V = -\delta_{cn}$ is the energy region in which the atoms are free atoms throughout the bulk. $U_{on} = U_{os}$ is assumed.

Cases (i)-(iii) below show further experimental indications of the superfluid bond.

(i). The λ specific heat   The superfluid bond excitation upon a global perturbation is directly indicated by the experimentally observed λ- C_V of He II between about 0.6 to 2.17 °K (circles, FIG. 3b).[85,86] For if the superfluid to normal fluid conversion, which occurs in large quantity here, energetically involves the conversion of Δ_b to the qualitatively smaller vdW bond of the normal fluid (FIG. 4a,b), then inevitably a large excess of heat supply is required. The activation energy, denoted by Δ_{sn}, is thus consumed mainly for Δ_b and, additionally for a site creation energy δ_{vn} and the kinetic energy E of a normal fluid He atom. Hence,

$$\Delta_{sn} = \Delta_b + \delta_{vn} + E. \tag{2a}$$

Using (2a), the thermodynamic evaluation in Sec. IX will justify the excitation scheme above to actually reproduce the experimentally observed λ-C_V: $\propto \exp(-\frac{\Delta_{sn}}{k_B T})$.

Furthermore, the Δ_b excitation scheme is supported by the observation that, a qualitative bonding change when transforming from one phase to the other is the common underlying excitation scheme for the second order phase transitions of a variety of systems (e.g. alloy) with a λ specific heat.

(ii). The dynamic structure factor about q_b   The superfluid bond excitation upon a local perturbation is directly pointed to, in the first instance, by the peculiar features in the $S(q_b, \omega)$, at $q_b \simeq 1.93$ Å^{-1}, of the superfluid (FIG. 1b).[15,67,70,89,90] Two of these are: 1) it peaks at a finite ω, $\omega(q_b) = \Delta_s \simeq 8.6$ °K which is basically independent of T. 2) its peak width is qualitatively narrow and on the T axis exhibits a sharp edge at T_λ.[67] By contrast, the peak of $S(q, \omega)$ of He I is broad, and its position diminishes towards zero as T rises, e.g. to ~4.5 °K/atom at $T = 2.9$ °K.[70] On the other hand, a simple cubic crystalline solid, for example, would show a zero frequency at q_b. The underlying Δ_b dynamics for the above is explained below. At q_b, which reciprocal being $\simeq 3.3 = a$ Å as noted earlier, the solution for the equation of motion (Eq. 12) relative to ξ, the dotted line in FIG. 1b, gives no phonon excitation. And, in real space, as viewed by a neutron committing a momentum exchange of $q_b = K_b$, all atoms are located at the bottoms of their potential wells; cf. Sec. V B(ii). Hence, when a He atom here is knocked by a neutron transferring an energy Δ_s just a fraction larger than the well depth $|U_{s0}| \sim \Delta_b$ (FIG. 4a), it is, if moved at all, knocked to just a fraction above the well. Then, the Δ_s is mainly consumed to excite the Δ_b and in addition, for a small site creation energy δ_s. As similar to Eq. (2a), we therefore have:

$$\Delta_s = \Delta_b + \delta_s. \tag{2b}$$

As the superfluid atoms are localized, $-\Delta_b$ and δ_s are therefore relatively sharply defined except for a finite smearing, primarily in δ_s, due to the short-range-ordering resultant fluctuations in the instantaneous atomic configuration. This therefore necessarily explains the

qualitatively narrower peak in $S(q, \omega)$. On the other hand, a finite smearing implied above is indeed supported by neutron scattering experiments which have shown the $S(q, \omega)$ peak – though narrow – has a finite width (e.g. systematically presented in FIG. 8 of Ref. 67), being a couple of times the instrumental resolution as used e.g. in Ref. 73, and being also at least several times wider than Landau's theoretical prediction based on roton-roton collisions. In contrast, in a normal fluid the essentially free atomic diffusion results in a significantly broad peak in the $S(q, \omega)$.

The Δ_b dynamic scheme is further supported by the third feature in the $S(q_b, \omega)$, namely that its intensity is the highest compared to at other q values. From the experimental data of Refs. 70, 68, the relative intensity, i.e. the ratio of the intensities, I_1 and I_2, below and above T_λ respectively is estimated to be 14 at q_b (FIG. 1c), which is about two times the second highest intensity, $I_1/I_2 \simeq 7$, at $q = 1.1$ Å^{-1}. An amplification of the scattering amplitude at q_b is to be expected, if an incident beam of monochromatic neutrons are indeed scattered by single atoms from an array of plans at a mean separation a, at which the condition $q_b = 2\pi/a$ implies an effective Bragg scattering (see further Sec. VIII).

That the same dynamics underlies both the λ specific heat and the excitation at q_b, as implied in (i) and (ii), can be justified by the fact that the latter indeed constitutes the major contribution to the former, as is shown both by our thermodynamic result, Sec. IX, and by the accurate numerical calculations of Yarnell[91] and others.[92] It is noteworthy that, a frequency dispersion with such a minimum at q_b was initially devised by Landau in his well known 1941 paper, in order to yield a λ specific heat. We here see that, the correspondence between the C_V and the $\omega(q)$ does not necessarily imply "which" dynamics.

(iii). The ion mobility The Δ_b dynamics scheme upon local perturbation is indicated, in the second instance, by the experimentally observed behaviour of the He ion mobility μ in He II,[93–95] which obeys

$$\mu = v_i/|\mathbf{E}|_a \propto \exp(\Delta/k_B T), \tag{3}$$

$\mathbf{E}_a$ being the applied field. Since by definition mobility is inversely proportional to the ion scattering rate and hence to the excitation probability $P \propto \exp(-\Delta_s/k_B T)$ (Sec. V D): namely it is $\propto 1/P \propto \exp(\Delta_s/k_B T)$, which is just as represented by Eq. (3). Hence the Δ of (3) identifies with the excitation energy, which is determined in the experiments to be 8.1 °K (for negative ions) or 8.8 °K (for positive ions). v_i is the ion drift velocity, having a magnitude typically $10 \sim 100$ m/sec. Clearly, the ion has a much higher kinetic energy than the thermal drift motion of a helium atom which velocity is in the order of 10^{-10} m/sec (see Sec. V C). Hence in the ion drifting process, the ion is essentially not subject to a many-quantum-atom correlation; and also the ion principally will transfer its energy and momentum to the superfluid, similar to the thermal neutron scattering. Hence, as discussed in (ii), the scattering is due to the Δ_b excitation. Indeed, the basically equality of Δ ($\simeq 8.1 \sim 8.6$ °K) from the ion scattering and the Δ_s of neutron scattering (Sec II B(ii)) further supports the Δ_b dynamics scheme.

The excitations in the two environments discussed in (i) and (ii)-(iii) can be generalized to be

$$\Delta_{s\alpha} \simeq \Delta_b + \delta_\alpha + E_\alpha, \tag{2}$$

α omitted for the local perturbation, $\alpha = s$, and n for the local and the massive bond break-up, $E_\alpha = <\epsilon> \simeq 0$ is the thermal kinetic energy of a He atom in the superfluid, and $E_\alpha = E$ in the normal fluid of He II. Using in (2b) the known values of Δ_s and Δ_b and with $E_s \simeq 0$ gives $\delta_s = 8.6 - 7.2 = 1.4$ °K.

C. The composition structure of He II, the momenton wave and the collective phonons

The realization of the relative localization of the superfluid atoms (Sec. II A), and the formation and preservation of their large bonding (to be justified in Sec. II B) and its

11

many-atom correlation origin (Sec. III), all point to a composition structure of the two-fluid coexistent as described with a **momenton** model (FIG. 5):

A **momenton** is firstly an aggregation of a large number of superfluid atoms, of an irregular shape and size of macroscopic scale. The motions of the atoms in it are primarily the $\mathbf{u}(\mathbf{R})$- oscillations as described in Sec. II A, which are about sites $\mathbf{R}$'s fixed in the center-of-mass coordinates of the momenton, $\boldsymbol{\xi}$, here. The two-fluid coexistent of He II consists of tremendously many momentons adjacent to the normal fluid regions, or within large (pure) superfluid regions. Dynamically as a whole, in a He II in thermal equilibrium at rest, each momenton oscillates slowly with an amplitude $\boldsymbol{\xi}(\boldsymbol{\Xi})$, about its equilibrium position, $\boldsymbol{\Xi}$; this motion is equivalent to the *simultaneous* and *in-phase* oscillations of all of the atoms in it, which (being of a small proportion) are superposed to the prominent coherent, not-in-phase $\mathbf{u}$ oscillations of the single atoms of Sec. II A. Under a pressure difference, $\boldsymbol{\Xi}$ describes the translation of a momenton, and hence the steady flow motion in the absence of convection. Finally, the excitation of a momenton occurs via the creation/annihilation of **collective phonons**, giving rise to the **momenton waves**.
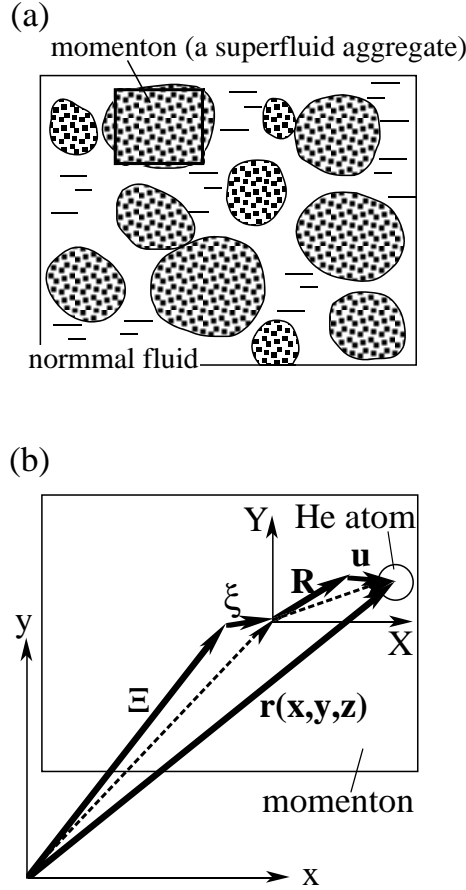
(a)

(b)

FIG. 5. (a). A snapshot of the schematic composition structure of He II at a T at which both fluids have a significant fraction. Each superfluid aggregate, a dotted region, represents a momenton; the momentons are randomly distributed through a normal fluid background. (b). In a momenton region, out of the thick framed region in (a), the absolute coordinates $\mathbf{r}$ of a superfluid atom is represented by the vector sum of four relative coordinates: $\mathbf{u}$ describes the atomic oscillation relative to $\mathbf{R}$, $\mathbf{R}$ the translation of the equilibrium position of the atom viewed from ξ, the coordinates of the center-of-mass of the momenton, ξ the oscillation of the momenton relative to $\boldsymbol{\Xi}$, and $\boldsymbol{\Xi}$ the translation of the equilibrium position of the momenton.

In contrast, *a mixture of two fluids which are intermingled on an atomic scale,* as is assumed in all of the existing models (or, the LLBF theory), lacks the mechanism for the preservation of the interaction of the respective fluids. The formation of momentons also is energetically favourable in two ways: 1) given the large superfluid atomic binding originates from a many-quantum-atom correlation (Sec. III), the gathering together of the superfluid atoms will allow an optimum atomic attraction, thus yielding the lowest energy of the system. 2) it requires less energy to turn a normal fluid atom into a superfluid atom, if the former is at the edge of the existing superfluid region rather than inside the normal fluid. Furthermore, based on the momenton model of composite structure, the two-fluid fractions can be quantitatively predicted with only the experimental density of liquid helium as an input data (Sec. IV), in satisfactory agreement with the statistical thermodynamics treatment in Sec. IX.

Direct experimental indications of the momenton wave include: (i) A slow propagation of the elastic wave – the so-called second sound wave – has been observed, e.g. by Peshkov et al.[65] and Atkins et al.,[96] in thermal pulse transmission measurements of He II. It occurs only at low frequency (less than 1000 cycle/sec); it has a slow propagation velocity, $c_2 \simeq$ 20 m/sec within 2.17 ~ 1 °K, and from about 1 °K downwards, c_2 increases rapidly and the pulse becomes substantially broadened. Despite the broadening, a finite width of the pulse is observed even with T being as low as 0.7 °K, which tends to suggest a finite size of the momenton in the superfluid. (ii). The thermal conductivity in He II[16] is observed to be abnormally large and not defined by a temperature gradient. The momenton wave essentially describes the phenomena of (i)-(ii). For instance, the simultaneous and in-phase oscillation of many atoms (of a momenton) in effect will produce the instant propagation of a heat pulse; in other words, the pulse is at once carried forward by a distance having the dimension of a momenton.

III. THE ORIGIN OF THE SUPERFLUID BOND

The experimental evidence of Secs. II A-II B together points to the cooccurrence of the large atomic bonding and the (relative) localization of the atoms in the superfluid. Such a cooccurrence commonly takes place in such processes as liquid solidification, for which the physics is generally understood. On the other hand, the physics for the superfluid atomic localization, which occurs uniquely as a result of the transformation from the classical state He I to the quantum fluid He II, appears specific. From the basic fact that the superfluid atoms are quantum mechanical, we can infer their enhanced bonding mechanism as follows. A quantum (fluid) atom is marked by a broadly spread wavefunction $\psi(\mathbf{r})$, through a volume at least a few times greater than a (see Sec. V). In this volume, at any location we will find a fractional density of atom A, $\psi_A^2(r_{A_i})$ and that of atom B, $\psi_B^2(r_{B_j})$; for simplicity, we call them partial-atom A_i and partial-atom B_j. Each partial atom consists of a fractional nucleus (of a charge $\psi^2(r)Z^{2+}$) and a fractional electron cloud (of a charge $\psi^2(r)Z^{2-}$) in just the way as the complete He atom, except for each being weighted by the fractional density $\psi^2(r)$ ($\int_V \psi^2(r)d\mathbf{r} = 1$.) The above yield three characteristics in the atomic interaction. 1). the exchange-correlation is amongst all of the partial-electrons of all of the partial-atoms, as well as among all of the partial nuclei, that tend to approach the same locations. In this complicated correlation process, the surrounding atoms extending to many neighbors are strongly involved with one another. 2). given an AB atom pair (meaning A sitting to the left of B), some of the partial-atom pairs can assume the $B_j A_i$ configurations. These $B_j A_i$ pairs will repel with each other when A and B are tending to part. Both of the above aspects will lead to the observation that the atoms are prohibited from separating from one another and are thus driven into a (relative) localization. 3). the interaction strength between a pair of partial-atoms is only a fraction of that of the total AB interaction. This will particularly affect, actually soften, the short-range repulsion.

In addition, the localization allows a cooperative motion of many helium atoms, the LAO scheme. The atomic polarizations are therefore induced systematically, which essentially corresponds to the London or dispersion energy,[97,98] of the form $e^4 h\nu_0/2\alpha^2 r^6$, rather than randomly as with the normal fluid van der Waals interaction.

IV. QUANTITATIVE DESCRIPTION OF THE COMPOSITION STRUCTURE OF He II, THE TWO FLUID FRACTIONS

Consider a He II bulk at a given T of the composite structure as depicted in Sec. II C; let the ith superfluid (s) or normal fluid (n) region in it be denoted by V_{si} or V_{ni}. Then one expects that the s and n component each has its own specific density, denoted by ρ_s and ρ_n. Incorporating further the factor that the atoms of the normal fluid are classical and of the superfluid are quantum mechanical, the local density of He II, i.e. the number of atoms per unit volume at $\mathbf{r}$ is thus

$$\rho(\mathbf{r}, T) = \begin{cases} \rho_s(\mathbf{r}, T) = \sum_j |\psi_s(\mathbf{r}_j)|^2, & \mathbf{r}_j, \mathbf{r} \in V_{si}, \\ \rho_n(\mathbf{r}, T) = \rho_n \delta(\mathbf{r}_j), & \mathbf{r}_j, \mathbf{r} \in V_{ni}, \end{cases} \tag{4}$$

or,

$$\rho(\mathbf{r}, T) = \rho_s(\mathbf{r}, T)\delta(\mathbf{r} \in V_{si}) + \rho_n(\mathbf{r}, T)\delta(\mathbf{r} \in V_{ni}). \tag{4$'$}$$

where $\psi(\mathbf{r}_j)$ and $\delta(\mathbf{r}_j)$ are the wavefunctions of a quantum and a normal helium atom respectively. The $\sum_j$ runs over all the atoms within the wavefunction overlap region including $\mathbf{r}_j = \mathbf{r}$.

We can define the volume fractions of the s and n fluids respectively by

$$f_s(T) = \frac{\sum_i V_{si}}{\sum_i V_{si} + \sum_i V_{ni}} = \frac{V_s}{V}, \qquad \text{and} \tag{5}$$

$$f_n(T) = 1 - f_s(T) = \frac{V_n}{V}, \tag{6}$$

where the sums cover all of the regions of the respective fluids in the container, and V, V_s, and V_n are the total volumes of the two-fluid mixture, the s and the n fluid, respectively. The average density of the two-fluid mixture is therefore

$$\begin{aligned} \rho(T) &= (1/V) \int_V \rho(\mathbf{r}, T) d\mathbf{r} \\ &= f_s(T)\rho_s(T) + f_n(T)\rho_n(T), \end{aligned} \tag{7}$$

where, the average densities of the respective fluids are

$$\rho_t(T) = \frac{N_t}{V_t} = (1/V_t) \int_{V_t} \rho_t(\mathbf{r}, T) d\mathbf{r}, \qquad t = s, n. \tag{8}$$

Based on Eqs. (5)-(7) we now determine $f_s(T)$ and $f_n(T)$ using only the experimental densities of liquid ^{4}He[99] as input data. Based on the close resemblance of the superfluid to a solid in a few important ways, e.g. as is shown by the essentially T independent thermodynamic functions (Sec. IX), we can assume that ρ_s is basically independent of T on the scale of concern, and can then write $\rho_s \approx \rho(0)$, $\rho(0) (= 0.1450 \text{ g/cm}^3)$ being the He II density at zero Kelvin. To obtain the ρ_n of He II, we next extrapolate $\rho_n(T)$ of the He I phase into the He II phase region using the thermal expansion function:

$$\rho_n(T) = \frac{0.1495}{\left(1 + 0.001603T - 0.002035T^2 + 0.001219T^3\right)^3}. \tag{9}$$

Where, the numerical coefficients are obtained from a least squares fit (solid line, FIG. 6a) to the experimental $\rho(T)$ data of He I (circles) between 2.6 to 4.4 °K. Substituting into Eq. (7) with the experimental $\rho(T)$ and the extrapolated $\rho_n(T)$ given in Eq. (9) for $T < 2.17$ °K, and by further combining with Eqs. (5)-(6), we then obtain for He II

$$f_s(T) = (\rho(T) - \rho_n(T)) / (\rho_s - \rho_n(T)) \tag{10a}$$

$$= \frac{\rho(T) - \frac{0.1495}{(1+0.001603T-0.002035T^2+0.001219T^3)^3}}{0.145 - \frac{0.1495}{(1+0.001603T-0.002035T^2+0.001219T^3)^3}}$$
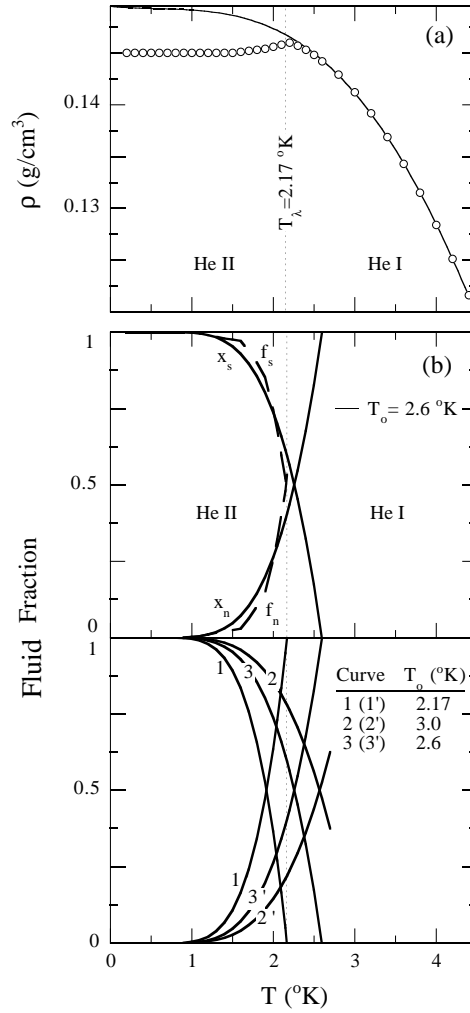
and $\quad f_n(T) = 1 - f_s(T),$ \hfill (10b)

FIG. 6. (a). The density $\rho_n(T)$ of the normal fluid component of He II, solid line within $T < T_\lambda$, as is extrapolated using the thermal expansion function Eq. (9). The coefficients are determined by a least squares fit to the experimental data of $\rho_n(T)$ (circles) 99 between 2.6 - 4.4 °K. (b). The volume fractions $f_s(T)$ and $f_n(T)$ of the superfluid and the normal fluid of He II, dashed curves, as given by Eq. (10), Sec. IV, established based on the composite structure of He II, namely large separate aggregates of the two fluids, and with the experimental density of He II as input. The number fractions x_s and x_n of the superfluid and the normal fluid of He II, solid lines, obtained from thermodynamic evaluation using Eqs. (70)-(70)′, Sec. IX. The lower and upper limits, solid lines 1 and 2, are obtained using $T_o = 2.17$ and 3.0 °K, and the optimum values, solid lines in the upper graph and solid lines-3 in the lower graph of (b), are obtained using $T_o = 2.6$ °K.

where all densities are in g/cm³. The resulting $f_s(T)$ and $f_n(T)$ (dashed lines in FIG. 6b) vary rapidly with T from about 50 % to 100 % and conversely between 2.17 - 0.6 °K, and approach to constant below 0.6 °K. In comparison, by Eq. (9) $\rho_n(T)$ and $\rho_s(T)$ vary by less than 4 % across the entire T range of He II. Combining the above features with (7), we therefore obtain that the T-dependence of $\rho(T)$ throughout the transition in 0.6-2.17 °K is principally determined by the variations in $f_s(T)$ and $f_n(T)$ with T. It is further particularly noticeable that at T_λ, f_s (~ 0.5) and f_n (~ 0.5) are not zero and one. The approximations involved would not cause any significant error as has been tested; rather, the non-unity of the fractions at the T_λ is plausibly as a consequence of the second order

phase transition. For, in such a transition a measurable n to s conversion begins to occur at a T, denoted by T_o, well above T_λ; that is, $f_s(T_o) = 0$ and $f_n(T_o) = 1$. The physics involved will be further clarified in Sec. X. The $f_s(T)$ and $f_n(T)$ obtained above are in good agreement with the thermodynamic results for x_s, x_n in Sec. IX, the resulting specific heat and entropy obtained based on which are in good agreement with experimental data; and these are consistent with the characteristic variation across the He II temperatures exhibited by a variety of properties of He II, including specific heat, and second sound.

V. EQUATIONS OF MOTION, THE SOLUTIONS, AND THEIR USE FOR DIRECTLY PREDICTING PROPERTIES OF HE II

A. The equations of motion via coordinate decomposition

The experimental evidence discussed in the preceding sections has pointed to the separate manifestations of the superfluid atomic dynamics with differing time and energy scales. Namely, a momenton oscillation, being of the scale of $\sim 10^3$ cycles/sec, is negligibly slower compared to the single atomic oscillation with respect to $\boldsymbol{\xi}$, typically of the scale of 10^{11} cycles/sec, so that the former can be regarded as being stationary within the oscillation cycle of the latter. Furthermore, the diffusion rate of the helium II atoms, with a diffusion constant $\sim 10^{-8}$ cm^2/sec. (cf. Sec. V C), is negligibly slower compared to the single atom oscillation rate, and will on the other hand neither effect the momenton oscillation. We now establish the equations of motions accordingly via decomposing the total motion in a similar way to the above. First, we may express the absolute position $\mathbf{r}$ of an atom with the vector sum

$$\mathbf{r}(x, y, z) = \mathbf{u}(u_x, u_y, u_z) + \mathbf{R}(X, Y, Z) \tag{11}$$
$$+\boldsymbol{\xi}(\xi_x, \xi_y, \xi_z) + \boldsymbol{\Xi}(\Xi_x, \Xi_y, \Xi_z),$$

where $\mathbf{u}$ is the displacement of a He atom relative to $\mathbf{R}$, $\mathbf{R}$ is the equilibrium position of the atom with respect to $\boldsymbol{\xi}$, $\boldsymbol{\xi}$ is the displacement of the center-of-mass of a momenton relative to $\boldsymbol{\Xi}$, and $\boldsymbol{\Xi}$ is the equilibrium position of the momenton with respect to the laboratory system (FIG. 5b). Accordingly, the total interatomic potential is $V(\mathbf{R} + \mathbf{u}) + \mathcal{V}(\boldsymbol{\Xi} + \boldsymbol{\xi})$, with the 1st and 2nd terms being due to the atoms, as viewed from $\boldsymbol{\xi}$, and the momentons. As discussed above, the relative coordinates are effectively decoupled, meaning $\partial \mathbf{r}/\partial x = \partial \mathbf{u}/\partial x + \partial \mathbf{R}/\partial x + \partial \boldsymbol{\xi}/\partial x + \partial \boldsymbol{\Xi}/\partial x$, etc. Hence, we obtain four separate equations of motions for an atom at site l of mass m and an momenton j of mass M_j, which in the semi-classical form formally are the Newton equations:

$$\mathbf{F}_l = m \frac{\partial^2 \mathbf{u}_l(K, t)}{\partial t^2} \tag{12a}$$

$$\mathbf{F}_R = m \frac{\partial^2 \mathbf{R}_l(K_b, t)}{\partial t^2}, \tag{13a}$$

$$l = 1, 2, \ldots$$

$$\mathbf{F}_\xi = M_j \frac{\partial^2 \boldsymbol{\xi}_j(K_M, t)}{\partial t^2}, \tag{14a}$$

$$\mathbf{F}_{\boldsymbol{\Xi}} = M_j \frac{\partial^2 \boldsymbol{\Xi}(k_s, t)}{\partial t^2}, \tag{15a}$$

$$j = 1, 2, \ldots.$$

Quantum mechanically the total Hamiltonian and the wavefunction are

$$H = H_u + H_R + H_\xi + H_\Xi, \tag{16}$$
$$\psi(\mathbf{r}) = \varphi(\mathbf{u})\phi(\mathbf{R})\Phi_\xi(\boldsymbol{\xi})\Psi_\Xi(\boldsymbol{\Xi}). \tag{17}$$

Here H_u, H_R, H_ξ and H_Ξ, and φ, ϕ, Ψ_ξ and Ψ_Ξ are the Hamiltonians and wavefunctions in the respective coordinates, $\mathbf{u}, \mathbf{R}, \boldsymbol{\xi}$ and $\boldsymbol{\Xi}$. The counterparts of Eqs. (12) - (15) are the Schrödinger equations:

$$H_u\varphi = \epsilon(K)\varphi \tag{12b}$$
$$H_R\phi = \subset (K)\phi \tag{13b}$$
$$H_\xi\Phi_\xi = \in (K_M)\Phi_\xi \tag{14b}$$
$$H_\Xi\Phi_\Xi(\boldsymbol{\Xi}) = e_s(k_s)\Phi_\Xi(\boldsymbol{\Xi}). \tag{15b}$$

In Secs. V B-V E we set up explicitly for the above equations and solve, and based on the solutions predict a few immediate properties of the system.

B. Cooperative oscillation of single atoms and single phonon excitation

1. Set-up of Eqs. (12a)-(12b)

Consider in the $\boldsymbol{\xi}$ coordinates the superfluid atoms are, as discussed in Sec. II A, localized and each oscillates about its equilibrium site $\mathbf{R}(X, Y, Z)$ along a chain of atoms say in the X direction, in a potential well $V(X)$ (FIG. 4a). The mean separation of the atoms is a; as based on the q_b (Sec. II), $a = 2\pi/q_b = 3.3$ Å. The complete oscillation motion can be projected along three orthogonal chains in X, Y, Z directions, which can be oriented in an arbitrary direction as the fluid is isotropic. In three dimension the dynamics above can be accordingly represented for a simple cubic *pseudo* lattice (see also Sec. II), which we shall use below, of an apparent and effective lattice constants, a and a_r (to be explained below), respectively, with one atom per unit cell. When needed, the effect of fluctuation about a may be plugged in e.g. by damping the average result obtained this way. As the fluid has no shear elasticity, the different parallel atomic chains are not correlated in motion or coordination; and along each chain only longitudinal waves present.

The exact many-body potential energy of an atom at X_l is $V(X_l + u_l)$, which is a function of the displacements of all (N_Υ) atoms within a correlation length Υ:

$$V(X_l + u_l(u_{l_\Sigma})) = V(X_l + u_l(u_{l_\Sigma}); u_{1_\Sigma}, u_{2_\Sigma}, \ldots, u_{N_\Upsilon,\Sigma}) \tag{18}$$

where $u_{l_\Sigma} = \sum_{l'} [(X_l + u_l) - (X_{l'} + u_{l'})]$ is the displacement of the atom at X_l relative to all other atoms in the chain. $V(X_l + u_l)$ expands into the Taylor series:

$$V(X_l + u_l) = V_0 + \frac{dV}{du_{l_\Sigma}} u_{l_\Sigma} + \frac{1}{2}\frac{d^2V}{du_{l_\Sigma}^2} u_{l_\Sigma}^2 + \ldots . \tag{19}$$

where V_0 is just the semi-classical ground-state potential energy with a zero-point energy effectively included; V_0 will not contribute to the force except when the motion of X_l is in question in which case it together with the $X_l(t)$ motion is then separately represented in Eq. (13a) In the LOD scheme, $\frac{dV}{du_{l_\Sigma}} u_{l_\Sigma}$ will average to zero for the atom oscillating about its equilibrium site. Because the superfluid bonding (Sec. III) has a large spatial extension, we expect that at larger u_l values, $\frac{d^2V}{du_{l_\Sigma}^2}$ varies only slowly with u_l, hence higher order terms than $d^2V/du_{l_\Sigma}^2$ are small altogether and can be neglected even at a relatively large u_l. $V(X_l + u_l)$ then reduces to the quadratic

$$V(u_l) = V_0 + \frac{1}{2}\frac{d^2V}{du_{l_\Sigma}^2} u_{l_\Sigma}^2 = V_0 + \frac{1}{2}\alpha_1 u_{l_\Sigma}^2; \tag{20}$$

where X_l, being inexplicit, is dropped for simplicity, $u_l = u_l(u_{l_\Sigma})$ and $\alpha_1 = \frac{d^2V}{du_{l_\Sigma}^2}$. For the many-body representation (18):

$$\alpha_1 = \frac{d^2V}{du_{l_\Sigma}^2} = \sum_{l'} \frac{\partial}{\partial u_{l'_\Sigma}} \left(\frac{dV}{du_{l_\Sigma}} \right)$$

$$= \sum_{l'} \frac{\partial^2 V}{\partial u_{l'_\Sigma} \partial u_{l_\Sigma}} \frac{\partial u_{l'_\Sigma}}{\partial u_{l_\Sigma}}, \tag{21}$$

where $\frac{dV}{du_{l_\Sigma}} = \sum_{l'} \frac{\partial V}{\partial u_{l'_\Sigma}} = \frac{\partial V}{\partial u_{l_\Sigma}}$ with all other terms cancelled out as the displacements altogether are symmetric about X_l. Taking derivative with respect to u_l on both sides of (20) we get the force acting on the atom at X_l:

$$F_l = \frac{dV}{du_{l_\Sigma}} = \sum_{l'} \frac{\partial^2 V}{\partial u_{l'_\Sigma} \partial u_{l_\Sigma}} \frac{\partial u_{l'_\Sigma}}{\partial u_{l_\Sigma}} \simeq -\alpha_1 u_{l_\Sigma}. \tag{22}$$

Eq. (22) or (21) contains only the non-zero, diagonal terms $q = q'$ ($q, q' = X, Y,$ or Z) of the block matrix components $\frac{\partial^2 V}{\partial u_{l'_\Sigma}^{q'} \partial u_{l_\Sigma}^q}$, representing the absence of shear elasticity of the fluid. Further we sum for u_{l_Σ} over only nearest-neighbors: $u_{l_\Sigma} = -u_{l+1} - u_{l-1} + 2u_l$. This together with the last expression of (22) represents an effective nearest-neighbor interaction and is used below; and the many-body correlation effect will be effectively included in an effective α_1 (or c_1) value determined by fitting to experimental data. With the u_{l_Σ} above in (22), and in turn (22) for F_l in Eq. 12a we get:

$$-\alpha_1(-u_{l+1} - u_{l-1} + 2u_l) = m\frac{\partial^2 u_l}{\partial t^2}, \qquad l = 0, 1, \dots \tag{12a$'$}$$

this being the independent harmonic oscillator description for the cooperative motion of the superfluid atoms in the $\boldsymbol{\xi}$ coordinates. It is noteworthy that, first, the averaging over many neighboring atoms in Eq. (21) results in an identical α_1 for all sites at all time, despite the reality that the physical parameters at each site in general fluctuate. This thereby leads to the well-defined, site-independent excitation energy as from Eq. (12a)$'$ (similarly Eq. (12b)). Second, F_l is a restoring force, either attraction or repulsion, as long as $\text{sign}(F_l) = -\,\text{sign}(u_{l_\Sigma})$, and further for the given $|F_l| \propto |u_{l_\Sigma}|$ here, $V(u_l) = -\int F_l du_{l_\Sigma}$ will then yield Eq. (20); we shall encounter this notion below.

From the above and using in advance the u_{l_Σ} expression from solving Eq. (12a) in Sec. V Bc, we have $V - V_0 = \frac{\alpha_1}{2}u_{l_\Sigma}^2 = \frac{1}{2}m\omega^2 u_l^2$, where $\alpha_1(K) = m\omega^2(K)$, and can then express for the total energy: $U_K = \frac{p_l^2}{2m} + (V - V_0)$ for the normal modes of each oscillator. The U_K, with $p_l = -i\hbar\frac{\partial^2}{\partial u_l^2}$, directly leads to H_u, with which in Eq. (12b) we have:

$$\left(-\frac{\hbar^2}{2m} \frac{\partial^2}{\partial u_l^2} + \frac{m\omega^2}{2} u_l^2 \right) \varphi(\mathbf{u}_l) = \epsilon(K)\varphi(\mathbf{u}_K) \tag{12b$'$}$$

2. Solution of Eq. (12b), single phonons and their wavefunctions

Equation (12b)$'$, which we here discuss first, has the well-known eigen energy solution:

$$\epsilon_n(K) = \left(n + \frac{1}{2} \right) \hbar\omega(K) \qquad n = 0, 1, 2, \dots, \tag{23}$$

which consists of n phonons, each having an energy quantum

$$\mathcal{E}(K) = \hbar\omega(K). \tag{24}$$

The stationary eigen functions are (here $u \equiv u_l$)

$$\varphi_n(u) = c_n H_n \left(\sqrt{\frac{m\omega}{\hbar}}\, u \right) \exp(-\frac{m\omega}{2\hbar}u^2). \tag{25}$$

18

H_n are the Hermit polynomials and c_n the normalization coefficients. The expectation value $< \epsilon_n >= \int \Phi_n^*(\mathbf{u},t)\epsilon_n\Phi_n(\mathbf{u},t)d\mathbf{u} = \sum_n \sum_K \epsilon_n(K)$, where $\Phi_n(u,t) = \varphi(u)\exp(\imath H/\hbar t)$ are the time dependent eigen functions, yields the total energy of the system, which will be given in Sec. IX by an ensemble average, the internal energy $U_s - U_{s0}$.

Equation (25) informs: 1) The spatial extension of $\varphi(u)$, as can be measured by $\Lambda_u = 2u|_{\varphi(u)=0.5\varphi(0)} = 2\sqrt{\frac{2\hbar}{m\omega}\ln 2}$, is large for the small helium mass. At a low energy, e.g. $\omega = 1$ °K, $\Lambda_{u_{He}} \simeq 8.2$ Å and is a few times larger than a. The minimum-energy (of the $\mathbf{u}$ motion) wavefunction $\varphi_0(u) = \sqrt{\frac{m\omega}{2\pi\hbar}}e^{\frac{m\omega}{2\hbar}u^2}$ at this ω is seen to extend into and beyond the first nearest-neighbor (solid curves, FIG. 4a2); and similarly with the excited states. By contrast, the wavefunction for an argon atom, of a mass $m_{Ar} \approx 10m_{He}$, (dotted curves in the figure) has $\Lambda_{u_{Ar}} \simeq 2.6$ Å, which is less than the interatomic spacing $a_{Ar} \simeq 5.3$ Å taken for solid argon. Λ_u, being a similar measure to the thermal de Broglie wavelength, thus defines that, (viewed now in $\boldsymbol{\xi}$) a helium is quantum mechanical and an argon classical. Λ_u increases with ω, but by Sec. V B 2 at a larger ω the atom is then confined in a narrower potential well; and at a high ω comparable to Δ_b the atom converts to the state of a normal fluid atom. 2) It follows from the large Λ_u that the single particle momentum of helium cannot be determined better than $\hbar/\Lambda_u$. 3) The immediate consequence of the large Λ_u, which causes the wavefunctions of several nearest-neighbor atoms or so to be entangled, is to result in the many-quantum-atom correlation scheme, and the consequent substantial superfluid bond and the localization of the He atoms, as discussed in Sec. III. 4) However, Λ_u is only several times a or so say within a region Υ; hence the helium atoms are "indistinguishable" effectively within only the limited Υ region ($\Upsilon <$ or $<< V$ of the container), in which the atomic wavefunctions overlap. This is in contrast to a free quantum particle whose uncertainty region consists in the entire volume of the particle assembly (the free electron gas is an example of such). Furthermore, since the atoms are localized and each can most probably be found about its equilibrium site, thus the individual atoms are not "identical" in respect of the sites they can occupy. Restating this condition, by regarding the localized atoms as being effectively "identical" instead, we have that the centres of mass of the atomic wave packets are effectively "distinguishable"; the atoms will become "effectively identical" if one views each "atom wavefunction + site"; the "independent harmonic oscillator" representation in this section is in effect a formal transformation to this status. Compare the discussion relevant to the R motion in Sec. V C.

3. *Solution of Eq. (12a), the dispersion curve for $q < 1.93$ Å^{-1}, and the potential energy*

Equation (12a) can be readily solved to give the oscillation amplitude $u_l(K) = Ae^{-\imath(la_\alpha K+\omega t)}$, thus $u_{l_\Sigma} = 4u_l\sin^2(\frac{Ka_\alpha}{2})$, and the normal-mode angular frequency and the $\mathcal{E}(K)$ by combining with (26) (both in J)

$$\omega(K) = \sqrt{\frac{\alpha_1}{m}} \ \ 2\sin\left(\frac{Ka_\alpha}{2}\right),$$

$$\text{and} \quad \varepsilon(K) = \mathcal{E}(K) = \hbar\omega(K)$$

$$\text{where}:$$

$$a_\alpha = \begin{cases} a, & K < 0.51, \text{ or } 1.87 < K < K_b - \frac{\sigma}{2}\text{Å}^{-1} \\ & \hspace{3.5cm} (26a) \\ a_r, & 0.51 \leq K \leq 1.87 \text{ Å}^{-1} \quad (26b) \end{cases}$$

For $K \lesssim 0.5$ Å^{-1} ($Ka << 1$), (26a) becomes

$$\mathcal{E}(K) \simeq \hbar c_1 K. \hspace{4cm} (26a)'$$

The phase velocity here is $\mathcal{E}/(\hbar K) = c_1 = \sqrt{\alpha_1/m}\ a$, being equal to the propagation velocity of the sound wave, $(1/\hbar)(\partial\mathcal{E}/\partial K)$. Parameterizing Eq. (26a) using the pulse transmission value 239 m/sec[76] for c_1, we get $\mathcal{E}(K) = 18.25K$ (°K) (solid line-1, FIG. 7a and also FIG.

19

1b) where K in Å^{-1}, in satisfactory agreement with the neutron-probed excitation curve[67] (circles) in this K region. The slope of the latter from a least squares fit is $c_1 = 238.9$ m/sec. The above result has been used as a fed-back information in Secs. II A-II B.
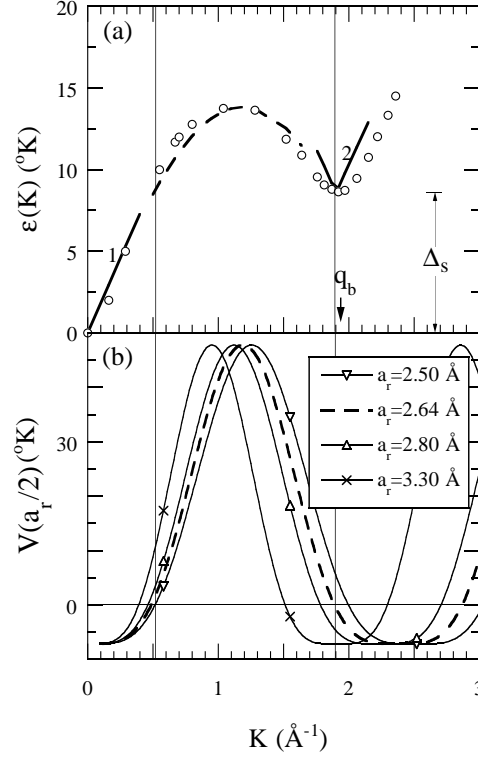

FIG. 7. (a) Theoretical total excitation energy $\varepsilon(K)$ versus phonon wavevector K of the superfluid of He II, solid and dashed curves. The excitation at a $K < K_b - \sigma/2$ is due to the creation of a single phonon, $\mathcal{E}(K)$ (solid curve 1), as predicted from the solution (26a-b) of the equation of motion of the He atoms performing independent harmonic oscillations relative to $\boldsymbol{\xi}$ in the potential wells $V(u)$ shown in FIG. 4. The above K region further divides into $K \lesssim 0.6$ Å^{-1}(Eq. 26a) and $< 0.6K < K_b - \sigma/2$ Å^{-1} (Eq. 26b), where the apparent parameter $a = 3.3$ Å and the effective $a_r = 2.64$ Å are, respectively, used as the interatomic spacing. In the vicinity of $K_b = 1.93$ Å^{-1}, i.e. $|K - K_b| < \sigma/2$, $\varepsilon(K)$ (solid curve 2) primarily results from the excitation of a superfluid bond, of an activation energy Δ_s, superposed with a small single phonon excitation energy: $\varepsilon(K) = \Delta_s(K) + \mathcal{E}(K)$, where $\varepsilon(K_b) = \Delta_s$. Neutron diffraction data points at 1.12 °K[67] are represented by circles. (b) Potential enenrgy of a superfluid atom, $V(u)$, as a function of K, Eq. (20)$'$ with $u = a_r/2$, plotted for several a_r values from 2.5 to 3.3 Å. At a fixed a_r, $V(\frac{1}{2}a_r)$ has a positive peak in a certain K region which shifts towards the higher K end with decreasing a_r. Only if $a_r \approx 2.64$ Å, the K region where $V(\frac{1}{2}a_r) > 0$ (dashed curve) coincides with the K region where $\mathcal{E}(K) > \Delta_s$ (dashed curve, FIG. 7a); this K region is bounded between (0.51, 1.87) Å^{-1} as indicated by the two dotted vertical lines.

For $0.5 \lesssim K \lesssim K_b(\equiv q_b)$ Å^{-1}, $\mathcal{E}(K)$ involves explicitly a_α and here $a_\alpha = a_r$. a_r, as an effective quantity of a, was introduced when setting up Eq. (12a)$'$ in order to now account for an apparent distortion of $\mathcal{E}(K)$ from the experimental curve if $a = 3.3$ Å is used in Eq. (26). For we recognize that, a helium atomic oscillator, having a broad wavefunction as Sec. V Bb showed, would overlap with its neighbours and hence repel each other at an effective border at $|\frac{1}{2}a_r| < |\frac{1}{2}a|$ (FIG.8). If the excitations indeed include oscillations of amplitudes larger than $\frac{1}{2}a_r$, then the finite oscillator size, reflected by the repulsion length AA' in FIG. 8, must be excluded from the apparent a. Thereby at these modes the atomic oscillator is effectively confined in $(-\frac{1}{2}a_r, \frac{1}{2}a_r)$. In resulting in a $\mathcal{E}(K)$ (dashed line in FIG. 7a and also FIG. 1b) in agreement with the experimental data in this K region, we find $a_r \approx 0.8a = 2.64$

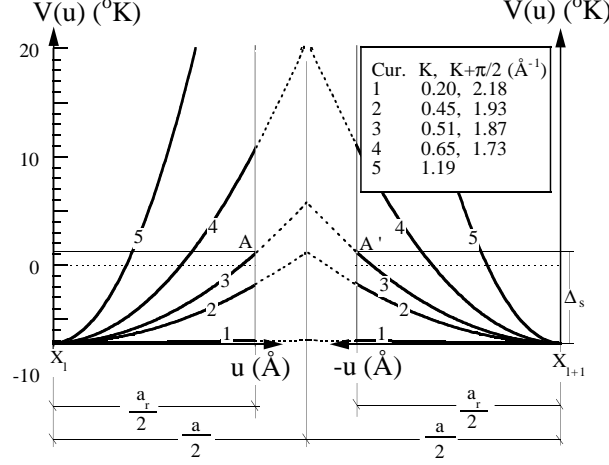Å. We will shortly justify that with this a_r value, $V(u)$ indeed turns to be > 0 at $u = \frac{1}{2}a_r$.

FIG. 8. Potential energy $V(u)$ versus u a of superfluid atom centered at X_l or X_{l+1}, Eq. (20)$'$ with $a_r = 2.64$ Å, plotted for several K values as indicated in the inset. For $K = 0.51$ Å^{-1}, from which towards higher K values $\varepsilon(K) > \Delta_s$ (see FIG. 7), the potential turns to be repulsive, i.e. $V(u) > 0$, at the effective border $u \pm \frac{a_r}{2}$ (curve 3). a is the apparent interatomic distance of He II as given by the reciprocal of K_b: $a = 2\pi/K_b = 3.3$ Å.

Using in Eq. (20)$'$ the $\alpha_1 = \frac{c_1^2 m}{a_r{}^2}$ as determined from the linear K region relation and the u_{l_Σ} expression, both just given, and with $V_0 \simeq U_{0s} = -7.2$ °K/atom as determined from experiment[88,18] (note that by letting $V_0 \simeq U_{0s}$ the zero point energy is effectively included; see also Secs. II B, IX) we have

$$V(u_l) = V_0 + \frac{1}{2}\frac{c_1^2 m}{a_r{}^2}u_{l_\Sigma}^2 = -7.2 + 31.6u_l^2 \sin^4(\frac{Ka_r}{2}), \qquad (20)'$$

where $V(u_l)$ is in °K, u_l in Å, and K in Å^{-1}; $a_r = 2.64$ Å for the parameterization; the resulting $V(u)$ for selected K values are graphically shown in FIG. 8. For $K < 0.51$ or $K > 1.87$ Å^{-1}, $V(u) < 0$ for all $|u|$ values up to $\frac{1}{2}a_r$. For $K = 0.51$ (or symmetrically 1.87) or $0.51 < K < 1.87$ Å^{-1}, $V(u)$ turns to be repulsive at $u = \frac{1}{2}a_r$ or earlier – we preassumed this in the preceding paragraph. Furthermore, the repulsive feature of $V(u)$ with K in $(0.51, 1.87)$ Å^{-1} is also precisely as expected from the excitation scheme derived in Sec. II. Namely, since in this K region the excitation energy $\mathcal{E}(K) > \Delta_s$ and $\mathcal{E}(K)$ corresponds to the $\max(|u|)$ for the given K, the $\mathcal{E}(K)$ here must therefore result from repulsion.

Compute $V(u_l)$ as a function of K with $u_l = \frac{1}{2}a_r$ in Eq. (20)$'$, for different a_r values from 2.5 to 3.3 Å. We find that at a fixed a_r, $V(\frac{1}{2}a_r)$ has a positive peak in a certain K region which shifts towards the higher K end with decreasing a_r (FIG. 7b). Only if $a_r \approx 2.64$ Å, the K region where $V(\frac{1}{2}a_r) > 0$ (dashed curve) coincides with the K region where $\mathcal{E}(K) > \Delta_s$ (dashed curve, FIG. 7a). Thus we have verified that the solution $a_r \approx 2.64$ Å is unique.

Furthermore we note that at $K = K_b = 1.93$ Å^{-1}, or $Ka = 2\pi$, all atoms move in phase: $u_{l+1}/u_l = \frac{\exp(l2\pi + \omega t)}{\exp((l+1)2\pi + \omega t)} \equiv 1$, and $u_{l_\Sigma} \equiv 0$. That is, in the K_b mode, in real space all atoms are at the bottoms of their potential wells as viewed, for example, by a neutron scattered due to this mode. The oscillations at the other normal modes would cause, with respect to the neutron, a snapshot of somewhat irregularly displaced "equilibrium sites" of the atoms which will add to their already irregularity due to a short range ordering.

Finally, the character of the localized oscillation of the helium atoms, being clearly distinct from that in solids, has up to now been represented in the formal treatments and are re-emphases as follows: it is relative to $\boldsymbol{\xi}$ rather than $\boldsymbol{\Xi}$, it is in cages fluctuating in location

and dimension, and it is in a shallow potential well which switches to repulsion at larger oscillation amplitudes.

C. Single atom translation and excitation of the superfluid bond

1. The semi-classical representation Eq. (13a), excitation of the superfluid bond

Equation (13a) describes, in a superfluid equilibrium in the absence of a pressure and composition gradient, the thermal fluctuation resultant translation (self-diffusion) of the equilibrium position $\mathbf{R}$ of a helium atom. This motion can be tracked by solving the simultaneous equations of motion for N atoms with an interatomic potential V_0, e.g. numerically with the help of computer. Macroscopically, the motion of, say, N' tagged atoms form a thermal diffusion flux of a concentration $c(\mathbf{R})$; the diffusion equation e.g. along X axis is

$$D \bigtriangledown^2 c(\mathbf{R}, t) - \frac{\partial c(\mathbf{R}, t)}{\partial t} = 0 \quad \text{(the macroscopic form).} \tag{13a}'$$

D, the diffusion constant, can be estimated by

$$D = Ca^2 \frac{\omega}{2\pi} e^{-\Delta_s k_B T}$$
$$\approx 2.4 \times 10^{-8} \qquad \text{cm}^2/\text{sec} \tag{26}$$

where C is the coordination number, $e^{-\Delta_s/k_B T}$ the Boltzmann factor and, by Sec. II B, Δ_s, =8.6 °K, is the activation energy of a superfluid bond. The numerical value of D is obtained using the previous values for a, and $\omega(= 10^{-9}$ 1/sec), with $\frac{C}{2\pi} \approx 1$ and $T = 1$ °K. This D value is as low as that of diffusion in a solid, informing that a superfluid atom is virtually localized. Accordingly the solutions of (13a) and (13a)$'$, of which $c(\mathbf{r})$ is known to be a Gaussian function, are not of interest here. D represents the probability for an helium atom to translate from its bonding state at $\mathbf{R}$ to that at a neighboring site at $\mathbf{R}'$ (which can statistically also be $\mathbf{R}$), by overcoming an energy barrier height $\Delta_b + \delta_v$ (FIG. 4a):

$$P(\mathbf{R} \to \mathbf{R}') \propto D \propto e^{-\frac{\Delta_{s\alpha}}{k_B T}}.$$

With He II, the $P(\mathbf{R} \to \mathbf{R}')$ processes of practical interest are ones caused by external perturbations, and in particular, the manifestations of the processes in the excitation spectrum which we discuss below, and in the specific heat which we discuss in Sec. IX.

Upon a local perturbation the excitation at $K = K_b$ is by Sec. II B(ii) due to activation of the superfluid bond:

$$\varepsilon(K) = \Delta_s = 8.56 \qquad (^o\text{K}) \qquad K = K_b \tag{26c}$$

And at a K apart from K_b but in a narrow vicinity $0 < |K - K_b| \leq \sigma$ is, by combining with Secs. II A and V B, therefore

$$\varepsilon(K) = \Delta_s(K_b) + \mathcal{E}(K) \approx 8.56 + 18.18|K - 1.93| \quad (^o\text{K}),$$
$$0 < |K - K_b| \leq \frac{\sigma}{2} \tag{26d}$$

Here, $\mathcal{E}(K) = \hbar c_1 |K - K_b|$ is the single phonon excitation energy of Eq. (26) after the simplification: $-\sin(\pi - \frac{Ka}{2}) \simeq -(\pi - \frac{Ka}{2})$ for $\pi - \frac{Ka}{2} << 1$. For the parameterization: $\Delta_s = \Delta_b + \delta_v = 8.6$ °K and $c_1 \simeq 239$ m/sec as given previously; K is in Å^{-1}. The resultant $\varepsilon(K)$ (solid line-2 in FIG. 7a and also FIG. 1b) agrees fairly well with the experimental curve, except for its hard turn at K_b as contrasted to the experimental smooth turn. This differnece is as expected, since the theoretical treatment does not include the effect of the fluctuation (resulting from a short range ordering) in the superfluid bond length which occurs in the real superfluid. Indeed, experimntal excitation data at high pressure ($\sim$25 atm)[100], which causes

a "solidification" effect, has shown a sharp turn at K_b similar to the theoretical description. (There are also shifts of the dispersion curve to a higher frequency and to a larger period, which can be understood similarly.)

As K departs from $(K_b - \frac{\sigma}{2}, K_b + \frac{\sigma}{2})$ to lower K values, the probability of the Δ_b excitation will drop rapidly, for the liquid density $n(\mathbf{r})$ drops as $\mathbf{r}$ departs from $\mathbf{R}$. So that $\varepsilon(K) = \mathcal{E}(K)$, which is the purely phonon excitation energy as of Eqs. (26a)-(26b).

2. The quantum mechanical representation Eq. (13b)

The potential energy for the R motion for a reference atom at R is:

$$\forall_0 (\leq 0) = \begin{cases} V_0 - \Delta_0, & |X| \leq \frac{a}{2} \\ 0, & |X| > 0, \end{cases} \tag{27}$$

Here Δ_0 is the zero point kinetic energy of the R motion; $V_0 = -7.2$ °K/atom as before. With $H_R = -\frac{\hbar^2}{2m}\nabla^2 + \forall_0$, $\forall_0$ as expressed above, in (13b) we have in the X direction

$$\left(-\frac{\hbar^2}{2m}\frac{d^2}{X^2} + \forall_0 \right) \phi = \subset \phi \qquad |X| \leq \frac{a}{2} \tag{13b$'$}$$

$$-\frac{\hbar^2}{2m}\frac{d^2}{X^2}\phi = \subset \phi \qquad |X| > \frac{a}{2}$$

The eigen function of an even parity is

$$\phi(X) = A\cos(KX), \qquad |X| \leq \frac{a}{2} \tag{28a}$$

$$\phi'(X) = Ce^{-K'|X|}, \qquad |X| > \frac{a}{2} \tag{28b}$$

where $\hbar K = \sqrt{2m(\subset + |\forall_0|)}$ and $K' = \frac{\sqrt{-2m\subset}}{\hbar}$. Applying the boundary condition at $X = |a/2|$, $\zeta \tan(\zeta) = K'(a/2)$, which, when substituted with the expressions for K and K' above, writes as $\eta \equiv \mathrm{ctan}(\zeta) = \frac{\zeta}{\sqrt{\beta^2 - \zeta^2}}$, with $\zeta \equiv K(a/2)$ and $\beta \equiv \sqrt{2m|\forall_0|}\,\hbar(a/2)$, the energy solution is given to be

$$\subset = -\frac{\hbar^2 \zeta^2}{2m(a/2)^2 \eta^2}. \tag{29}$$

Starting with a guess value for $\forall_0$ and thus for β, put $a = a_r = 2.64$ Å for the same reason as before, solve graphically for η and ζ, and thus $\subset$; use the resulting $\subset_0$ value in (31) (below) and Δ_0 in turn in (27) to acquire a new $\forall_0$ value; and execute this iteratively until $\forall_0$ reaches constancy. We find, for $\forall_0$ being small here there is only one, hence the ground state solution:

$$\forall_0 = -10.65 \ (^o\mathrm{K}), \qquad \text{thus } \beta = 1.749,$$
$$\eta_0 = 0.68, \quad \zeta_0 = 0.31\pi. \tag{30}$$

With the η_0 and ζ_0 values above in (29) we get the ground state eigen energy of the R motion:

$$\subset_0 = -7.13 \quad ^o\mathrm{K/atom} \tag{29$'$}$$

With the $\subset_0$ we further get:

$$\Delta_0 = \subset_0 - \forall_0 = 3.45 \quad ^o\mathrm{K/atom} \tag{31}$$

The solution of odd parity is discarded as it does not fulfil the requirement of a symmetric (ground state) wave function for identical boson particles (Sec. V B-2); see further Sec. V F.

D. Momenton oscillation and excitation of collective phonons

1. Set-up of Eqs. (14a)-(14b) and the solutions

Equations (14) are formally set up for every momenton masses, M_j, $j = 1, 2, \ldots$, with the inter-momenton potential $\mathcal{V}(\boldsymbol{\Xi} + \boldsymbol{\xi})$, in the independent harmonic oscillator approximation. Since the momenton contribution to the total energy and excitation is negligible (see below), we will not solve its exact motion here and will only look at its long wave propagation, using an average mass M and with an effective force constant α_2. Equations (14) thus reduce to a single equation similar to Eq. (12a)$'$; its energy solution is thus:

$$\mathcal{E}_2(K_M) \approx \hbar c_2 K_M, \tag{32}$$

where the wave number and velocity of a collective phonon are $K_M = 2\pi/\prod$, Λ_M being the momenton wavelength, and

$$c_2 = \frac{\partial(\mathcal{E}_M/\hbar)}{\partial K_M} = \sqrt{\frac{\alpha_2}{M}}\, L_M = \sqrt{\frac{\alpha_{21}}{m}}\quad a, \tag{33}$$

respectively. Apparently c_2 corresponds to the velocity of second sound discussed in Sec. II C; α_2, $M = (N_M)^3 m$, $L_M = N_M a$ and N_M are the restoring force constant, mass, dimension and number of helium atoms in one dimension of a momenton oscillator, respectively. $\alpha_{21} \simeq \alpha_2/N_M^3$ represents then the effective force constant between two He atoms at the interface of two momentons. $c_2(T)$ is dependent of T via:

$$\frac{dc_2(T)}{dT} = \frac{\partial c_2}{\partial N_M}\frac{\partial N_M}{\partial T} + \frac{\partial c_2}{\partial \alpha_{21}}\frac{\partial \alpha_{21}}{\partial T}. \tag{34}$$

Suppose at a higher T a momenton will most likely find itself immediately surrounded by normal fluid regions, the reduction of T is thus mainly to increase the number of momentons. Then N_M and α_{21} and, by Eq. 34 hence $c_2(T)$, are basically constant. Meanwhile, the interaction of a momenton with the surrounding normal fluid gives: $\alpha_{21} < \alpha_1$. Immediately this gives: $c_2 < c_1$. As T is reduced (to about 1 °K) such that with a falling T, each existing momenton increases in both L_M and in its adjacency with other momentons for which α_{21} enhances, i.e. $\frac{\partial N_M}{\partial T} << 0$ and $\frac{\partial \alpha_{21}}{\partial T} << 0$. Hence, by Eq. (34) $\frac{dc_2}{dT} << 0$. In other words, c_2 increases rapidly with falling T, this being consistent with the experimental observation discussed Sec. II C. Furthermore, as with Eq. (23), the momenton excitation energies are $\in_{\mathcal{N}} = (\mathcal{N} + 1/2)\mathcal{E}_M(K_M)$, where $\mathcal{N} = 0, 1, \ldots$, and $\mathcal{E}_M(K_M) = \hbar\Omega(K_M)$ is the energy quantum of a collective phonon. Typically $\mathcal{E}_M(K_M) \sim 7.6 \times 10^{-9}$ °K, as based on the upper-limit in the experimental second sound wave frequency, $\Omega \sim 10^3$ cycle/sec. Hence, $\mathcal{E}_M(K_M)$ is negligible compared to the typical energy scale of a single phonon, $\hbar\omega \sim 0.8$ °K ($\sim 10^{11}$ 1/sec). Accordingly the momenton oscillation amplitude $|\Phi_\xi(\xi)|^2$ would be basically constant on the scale of $|\varphi(u)|^2$ and can be dropped from (17). Finally, since Λ_M is large, a momenton wave will be absent in a small sample.

2. Momenton wave, the atomic dynamics of second sound wave and temperature fluctuation

Consider a given normal-mode frequency Ω of momenton oscillation that is equal to the normal-mode frequency ω of single-atom oscillation; the latter consists of all wavelengths (much shorter than the momenton dimension) within the momenton. Two extreme cases can present. With some momentons, the Ω periodic process is in phase with the ω oscillation. Evidently, the Ω wave of amplitude A_Ω, which will superpose with the ω wave of amplitude A_ω, will then increase the A_ω to $A'_\omega = A_\omega + A_\Omega$. And conversely with some other momentons. Therefore, in each of the former momenton regions the phonon population n and thus the temperature T are increased by small amounts $n' - n \propto 2A_\Omega A_\omega$ and $T' - T$, as $(A_\omega)^2 \propto n$, noting $A_\Omega << A_\omega$; and conversely in the latter regions. So that a temperature wave forms, which is one defining characteristic of the so-called second sound wave.[102]

E. Superfluid flow, translation of momentons or of single atoms as of Eqs. (15)-(15b)

Equation (15a) describes a steady flow motion of the superfluid in the absence of convection and is expressed for the translation of the equilibrium position Ξ of a momenton. Under normal friction conditions, the flow is driven by an external pressure difference $P_1 - P_2$ acting on a cross sectional area S of the flow, hence $F_\Sigma = (P_1 - P_2)S$. One portion of the F_Σ is used to overcome the viscous resistance from the channel wall f acting on the flow through a flow-wall contact area A_{sw}; and the remaining to accelerate the flow inertia, the flow mass, which is

$$M_s = \sum_i M_i = N_s m. \tag{35}$$

N_s is the total number of helium atoms in the flow, and m – as before – the atomic mass of helium. Because $< \mathbf{u} > = < \boldsymbol{\xi} > = 0$ and also $< \mathbf{R} > \approx$ constant ($\mathbf{C}$) ($<>$ denotes the time average of a variable over an infinitesimal flow translation), therefore

$$< \mathbf{r} > (t) \ = \Xi(t) \ + \mathbf{C}. \tag{36}$$

(36) implies that the translation of a single atom, or a momenton, or the flow, describes the same motion. If $f \approx 0$, which will occur when v_s is below a critical value (which criterion is given in paper II), Eq. (15a) then describes the non-dissipative superfluidity flow motion. F_Σ is then entirely consumed to accelerate the flow velocity, for example at time $t = \tau$, to $v_s(\tau) = (1/M_s) \int_0^\tau \left[\int_0^\tau (P_1 - P_2)S(t)dt \right] dt$. If from $t \geq \tau$, the driving pressure is removed: $(P_1 - P_2)|_{t \geq \tau} = 0$. Then Eq. (15) and its solution become simply

$$M_s \frac{\partial^2 < \Xi >}{\partial t^2} = m \frac{\partial^2 < \mathbf{r} >}{\partial t^2} = 0, \qquad \text{and} \tag{15a$'$}$$

$$v_s = \frac{\partial < \mathbf{r} >}{\partial t} = \frac{\partial < \Xi >}{\partial t} = v_s(\tau) \equiv \text{constant}. \tag{37}$$

The classical equation (15a) validly describes the motion of the center of mass of an atomic wave packet.

The translations of the quantum helium II atoms are more fully, or strictly, described by Eq. (15b). As $H_\Sigma = p^2/2m + V_\Sigma$ and $V_\Sigma = 0$ in the absence of non-uniform external field, the solution of (15b) is an "effective" planewave:

$$\Phi(< \mathbf{r} >) = Ce^{i(\mathbf{k_s} <\mathbf{r}> - \omega t)}, \tag{38}$$

with "effective" referring to the fact that each single atom, if driven externally, is accelerated according to the relation (15), to a velocity v_s with an effective mass equal to the flow mass M_s. The wave number k_s is connected with v_s by the de Broglie relation:

$$k_s = mv_s/\hbar; \tag{39}$$

k_s is thus similarly effective. The translation kinetic energy of an atom is accordingly $e_s = mv_s^2/2 = \hbar^2 k_s^2/2m$. The flow energy is thus: $E_s = \frac{1}{2}M_s v_s^2 = N_s e_s = N_s \frac{\hbar^2 k_s^2}{2m_s}$. It is noteworthy that, Eq. (39) holds only for the steady flow motion here, where periodical processes of each atomic waves are essentially linear, independent and hence obey the superposition principle of quantum mechanics. However, when some part (e.g. the interfacial layer) of the flow is being resisted as opposed the remaining part, the former will interact with the latter given that the superfluid atoms are strongly correlated. Then, each atom in respect of its flow motion is no longer a "free" particle.

By knowing v_s and the density $\rho_s = |\psi|^2$, with $\psi(r)$ as in Eq. (17) the superfluid current density is given accordingly

$$\mathbf{j}_s = \frac{\hbar}{i2m}[\psi^* \nabla \psi - (\nabla \psi^*)\psi] = \rho_s v_s. \tag{40}$$

For the two-fluid coexistent of He II under thermal equilibrium, by Sec. II C each of the fluids are maintained in their own regions with no intermingling on an atomic scale, therefore each fluid maintains its specific density. For a steady, non-compressible flow, the continuity conditions follow accordingly

$$\nabla \cdot \mathbf{j}_s + \frac{\partial \rho_s}{\partial t} = 0 \qquad \text{and} \qquad \nabla \cdot \mathbf{j}_n + \frac{\partial \rho_n}{\partial t} = 0. \tag{41}$$

For a steady superfluid flow in a straight channel, the above becomes $\nabla \cdot \mathbf{j}_s = \frac{\partial \rho_s}{\partial t} = 0$ and $\nabla \cdot \mathbf{j}_n = \frac{\partial \rho_n}{\partial t} = 0$. For a steady flow of a two-fluid mixture maintained by a pressure difference there is $v_s = v_n$, and the island-like composite structure (FIG. 5a) should then maintain. If now the driving pressure is removed, so that, starting from the layers by the wall, $v_n = 0$ and only the (pure) superfluid will flow. A natural course via which this actually takes place is that the superfluid will break through the normal fluid and re-shape itself into narrow strips.

F. The total and full excitation spectrum, the total wavefunction and total zero point energy

a. The total and full excitation spectrum. The total excitation energy for a superfluid at rest is

$$\begin{aligned}
\varepsilon(K) &= \mathcal{E}(K) + \Delta_b(K) + O(\mathcal{E}_M) \\
&\simeq \mathcal{E}(K) + \Delta_b(K).
\end{aligned} \tag{42}$$

The full spectrum of $\varepsilon(K)$ in (0, 1.93) Å^{-1} is combinatorially given by Eqs. 26a, b,c,d (solid curve 1, the dashed curve, and solid curve 2 in FIG. 7 and also in FIG. 1). The single phonon and the superfluid bond excitations are, as the evaluation of specific heat in Sec. IX will show, characteristic in the T regions (0, 0.6) and (0.6, 2.17) °K respectively.

b. The total zero point energy is:

$$\begin{aligned}
\exists_0 &= \epsilon_0 + \Delta_0 + O(\in_0) \\
&\simeq 7.5 + 3.45 = 10.95 \ {}^o\text{K/atom}
\end{aligned} \tag{43}$$

where ϵ_0 and Δ_0 are given by (76) and (31).

c. The total ground state potential energy is:

$$\begin{aligned}
\Phi_0 &= V_0 - \exists_0 = \forall_0 - \epsilon_0 - O(\in_0) \\
&= -7.5 - 10.5 = -18.5 \ {}^o\text{K/atom}
\end{aligned} \tag{44}$$

where $\forall_0$ is given by Eq. (30).

d. The total wavefunction. Of the $\psi(\mathbf{r})$, Eq. (17), for an atom at $\mathbf{r}(x, y, z)$, given the rapid $\mathbf{u}$ oscillation, say in the x direction, $\varphi(u(X))$ as of Eq. (25) will on the time scale of the R motion show as an time average to be an even function relative to X. $\Psi_\xi(\boldsymbol{\xi})$ is even both for a similar reason and because $|\Psi_\xi|^2$ is essentially flat (and shallow) within the region of wavefunction overlap. $\phi(X)$ of Eqs. (28a)- (28b) is even. Last, $\Psi_\Xi(\boldsymbol{\Xi})$ is identical for all atoms in the (flow) bulk. Hence, overall, on the time scale of R motion, by which the atoms may exchange positions on activation, $\psi(x)$ is an even function with respect to the equilibrium position X; and x can be an arbitrary direction relative to the isotropic fluid. Therefore, $\psi(x)$ is spherically symmetric about R. The product of the single particle wave functions therefore yields a desirable, symmetric total wave function of N identical (in the sense of Sec. V B-2) particles of the fluid bulk:

$$\Psi(r_1, r_2, \ldots, r_N) = \psi(r_1)\psi(r_2)\ldots\psi(r_N). \tag{45}$$

26

VI. THE STABILITY CONDITION OF THE SUPERFLUID

From the superfluid bonding character we can infer: 1). The substantial superfluid bond, being larger than the van der Waals "bond" of He I (quantitative evaluation given in Sec. IX), implies a substantial *internal viscosity*, larger than that of He I. Thus the superfluid is not an assembly of *non-interacting atoms* and hence cannot be of *a zero internal viscosity* – as portrayed in London's BEC and in the unified LLBF theory as well. Meanwhile, the "weakly" (or sometimes referred to as "substantially") interacting superfluid atoms" and the "zero viscosity" which are simultaneously held in the LLBF theory, are two inevitable self-contradictory aspects. 2). Now that the viscosity of liquid He I can sustain a non-turbulent macroscopic rotation (below certain velocity) of He I which is a commonplace experimental observation, the larger internal viscosity of the superfluid He II can therefore certainly ensure a (more robust) *non-turbulent* macroscopic rotation of He II. The superfluid is thus not *irrotational*. 3). It therefore also follows that for the superfluid a *zero total circulation*, $\kappa_{tot} = 0$, is not a necessary condition for non-turbulence; instead κ_{tot} is finite and quantized, as has been experimentally demonstrated and to which a consistent theoretical grounding is provided in Sec. VII. 4). Accordingly, no *local vorticity* needs be imposed on the superfluid, as the Stoke's theorem,[103] applying for a viscous-less fluid, does not apply to the superfluid. 5). It also follows from points 1)-3) that the grounds for proposing the "absence" of internal viscosity as an explanation for the non-dissipative superfluidity motion are lacking. (This is in addition to the fact that an internal viscosity does not necessarily imply which "flow-wall" viscosity, which we are however not to expand on here.)

VII. THE QUANTIZATION OF CIRCULATION

Consider a superfluid bulk in steady rotational flow motion with a tangential velocity v_s. The trajectory of a flow atom $< r >$, Eq. (38), can be now conveniently projected onto the circular coordinate ℓ along the flow streamline, $<>$ being here for simplicity omitted. The atomic wave, assuming being localized relative to the rotational frame and hence not to swapped off the stream line, in the circular loop, of a circumference $\overline{L}$, must satisfy according to quantum mechanics the continuity condition:

$$k_s \overline{L} = n2\pi. \tag{46a}$$

This then yields a circulation quantization as to be expressed in Eq. (49) below. The case here is seen to be equivalent to an electron wave orbiting about the nucleus, except for their different centripetal forces.

Alternative to the above, to examine its microscopic detail we below look at the process from the standpoint of wave interference. We first determine an important parameter, the length of the rotational wave train of a helium atom, and this in theory is simply

$$L_{\mathrm{w}} = N_\lambda \cdot \lambda_s \tag{47}$$

where λ_s is the wavelength and N_λ is the number of λ_s's of the rotational wave train. The de Broglie relation (39) informs about $\lambda_s = 2\pi/k_s$, and not the N_λ. As to the physical acquisition of L_{w}, let us think that the action of passing a $\hbar k_s$ to a helium atom consists in passing it a field – in the form of a (purely) rotational wave train – whose momentum equals $\hbar k_s$. [We are tempted to think of this field being an electromagnetic wave, although this link would require a justification which goes beyond the context of this paper.] Since this wave is given as the solution of the Schrödinger equation (15b), we shall merely take this consequence. We can then think of the total atomic wave train now rotating along ℓ as the stationary thermal de Broglie wave train of a helium atom as being superposed in the rotational frame onto the purely rotational wave train of length $\lambda_s \cdot N_\lambda$. The former, having a wavelength of typically nano meters, will not contribute to the interference of a macroscopic length period. Consider now only the latter; its N_λ is evidently determined by the interaction time, τ_{w}, taken for creating the purely rotational wave train. That is,

$\tau_{\mathrm{w}} = N_\lambda T_s$, $T_s = 2\pi/\omega_s$ being the time period of the wave (or the period of its generating source), and $\omega_s = 2\pi v_s/\lambda_s$. Clearly, for wave interference to occur at a low n number in Eq. (46), first of all λ_s needs be so large as to be comparable with $\overline{L}$. Given m, of the helium atom here, is large compared to that of the usual quantum particles such as the electron, an (arbitrarily) large λ_s $(= \hbar/mv_s)$ can be achieved by compensatorily making the flow velocity v_s (arbitrarily) small, thus the T_s and $\overline{L}$ being accordingly large. In experimentation, for instance, a large T_s value ranging $30 \sim 600$ seconds, with a $\overline{L} \sim 0.0025$ cm were achieved.[11] Furthermore, to achieve $n = N_\lambda > 2$ or $>> 2$, the τ_{w} should $> 2T$ or $>> 2T$.

If the above conditions are met. We can then achieve $L_{\mathrm{w}} = N_\lambda \lambda_s \geq 2\overline{L}$, with $N_\lambda \geq 2$. In this way, each rotational atomic wave train will wind about each loop at least twice, interference will now occur. For the loop satisfying

$$\overline{L} = 2n\frac{\lambda_s}{2}, \tag{46b}$$

where the $\overline{L}$ will sometimes also write as $\overline{L}_{2n}$ and n is as before an integer, then, the rejoining waves will be in phase:

$$\Phi(\ell_1') = e^{i(k_s\ell_1 + \oint k_s d\ell)} = e^{i(k_s\ell_1 + 2\pi n)} \tag{48}$$
$$= e^{ik_s\ell_1}(\cos 2\pi n + i \sin 2\pi n) = \Phi(\ell_1).$$

This gives an amplified total amplitude: $\Psi(\ell_1') + \Psi(\ell_1) = 2\Psi(\ell_1)$. Re-writing Eq. (48) in terms of circulation, κ_{rot}, we get:

$$\kappa_{\mathrm{rot}} = \oint v_s d\ell = \frac{\hbar}{m} \oint k_s d\ell = \frac{h}{m} k_s \overline{L} = \frac{nh}{m},$$
$$n = 0, 1, 2, \ldots . \tag{49}$$

that is, the circulation is quantized. Or, if $\overline{L} = (2n+1)\frac{1}{2}\lambda_s$, the amplitudes will cancel out: $\Phi(\ell_1) + \Phi(\ell_1') = 0$. The amplitudes will partially cancel if $\overline{L}$ is a fraction of λ_s and n is small (~ 2), but will cancelled out quite cleanly if $n >> 2$ in which case the partially out-of-phase waves are superposed a large n number of times. The above is a standing wave to the observer who rotates with the flow. Since all of the rational atom waves in the flow have identical v_s, m, and hence identical λ_s, and are also in phase (for they are set to rotation at the same time and they are relatively localized), thus they will all present amplified amplitudes at the same circumferences $\overline{L}$ defined by (46b), and zero elsewhere. In the former case, the linearly superposed atomic waves yield a total enhanced fluid density, presenting macroscopically discrete streamlines.

Finally, by Sec. VI, the macroscopic rotation following the vessel above is the only rotational motion, therefore the total circulation is $\kappa_{tot} = \kappa_{rot} = nh/m$, where $n = 0, 1, 2, \ldots$. The signal of a measurement, if being in proportion to the total amplitude of the atomic waves, will then inform a circulation quantization.

The physical process described above, which can be termed the **circular atomic wave self-interference**, provides a mechanism for the circulation quantization that has been experimentally demonstrated.[11−13,31]

VIII. THE DYNAMIC STRUCTURE FACTOR ABOUT Q_B AS DUE TO THE SUPERFLUID BOND EXCITATION

Corresponding to the total excitation energy $\varepsilon(K)$ (42), the total dynamic structure factor from a (pure) superfluid is

$$S(q, \omega) = S(q, [\mathcal{E}(K) + \Delta(K)]/\hbar) \tag{50}$$
$$= \begin{cases} S_{\mathrm{ph}}(q, \mathcal{E}(K)), & q < q_b - \frac{\sigma}{2} & \text{(a)} \\ S_{\mathrm{ph},b}(q, [\mathcal{E}(K - K_b) + \Delta_b]/\hbar), & |q - q_b| < \frac{\sigma}{2} & \text{(b)} \\ S_b(q, \Delta_b), & q = q_b & \text{(c)} \end{cases}$$

here σ represents a narrow vicinity of q_b. For the phonon excitation, $S_{\mathrm{ph}}(q,\omega)$, by Eq. (23) the ϵ_n's of the scattering system are discrete. Neglecting phonon-phonon collisions, which is to a good approximation as based on neutron scattering measurements (Sec II A) and thermal conductance measurements,[104] and as has also been theoretically evaluated by Cohen and Feynman,[105] it follows then effectively

$$S_{\mathrm{ph}}(q,\omega) \propto \delta\left(\omega(K) - \frac{1}{\hbar}\left(\epsilon_n(K) - \epsilon_{n+1}(K)\right)\right),\tag{51}$$

where $K = q (\equiv |k'_{\mathrm{ne}} - k_{\mathrm{ne}}|)$, k_{ne} and k'_{ne} being the wavevectors of a neutron before and after scattering.

At $q_b = 2\pi/a = b$, b being reciprocal pseudo lattice vector, by Sec. II B $S(q,\omega)$ is due to the excitation of a superfluid bond and is thus expressed by (50c). In $|q - q_b| < \sigma/2$ where when $S_b(q,\omega) >> S_{\mathrm{ph},b}(\omega,q)$, then (50b) writes $S_{\mathrm{ph},b} \approx S_b(q,\omega)$; a switching-over region where $S_b(q,\omega)$ and $S_{\mathrm{ph},b}$ may have similar weights but would be very narrow, and is not to be dealt with here. As Sec. II C reviews, $S_b(q,\omega)$ as measured by neutrons presents a peculiarly high and sharp peak centered at $\omega = \Delta_s/\hbar = 8.6$ °K. Below we formally express $S_b(q,\omega)$ through a few combinatory modifications from a crystalline solid scattering for which we have the precise description, to elucidate the route via which the superfluid has acquired this particular scattering feature, apparently differing from that of either a solid or a liquid.

(a). Let us start with an imaginary superfluid, in which the atoms are arranged in a periodic lattice of a simple cubic structure, and the atomic bonding and activation energies, denoted by Δ_b^{cry} and $\Delta_s^{\mathrm{cry}} = \Delta_b^{\mathrm{cry}} + \delta^{\mathrm{cry}}$, are as large as in a solid. For this system, (only considering the longitudinal modes) the excitation energy $\mathcal{E}(q)$ is regularly given by Eq. (26) to be a sinusoidal dispersion, the dotted line in FIG. 1a, which is zero at $q_b = b$. $\mathcal{E}(q_b) = \hbar\omega(q_q) = 0$ together with $q_b a = 2\pi$ implies that at q_b, $S_{\mathrm{ph}}(q_b,\omega) \equiv 0$ and an elastic Bragg scattering occurs. The scattering intensity at a given q is proportional to the static structure factor, which (strictly) at zero °K is

$$S^{\mathrm{cry}}(q) = \frac{1}{N}\sum_{i,j}^{N} e^{\imath \mathbf{q}\cdot(\mathbf{r}_i - \mathbf{r}_j)}$$
$$= \int \left[S_{\mathrm{ph}}(q,\omega) + S_b^{\mathrm{cry}}(q,\omega)\right]\delta(\omega)d(\hbar\omega)$$
$$= \hbar S_b^{\mathrm{cry}}(q,\omega)|_{\omega=0}.\tag{52a}$$

The first expression of (52a) is just the Bragg scattering condition; it gives $S^{\mathrm{cry}}(q) = 1$ at $\mathbf{q}\cdot(\mathbf{r}_i - \mathbf{r}_j) = q_b a = n2\pi$ ($n = 0, 1, \dots$) and zero elsewhere. The last two expressions of (52) generalize $S^{\mathrm{cry}}(q)$ to include an energy transfer ω but with $\omega = 0$ for the *elastic* scattering of the present system. The *elastic* feature is readily understood to result principally from the inequality:

$$\begin{array}{ccc} \frac{\hbar^2 k_{\mathrm{ne}}^2}{m_{\mathrm{ne}}} & << & \Delta_s^{\mathrm{cry}}, \\ (5 \sim 100 \text{ meV}) & & (1 \sim 10 \text{ eV for solids}) \end{array}\tag{53a}$$

where k_{ne} ($= m_{\mathrm{ne}}v_{\mathrm{ne}}/\hbar$), v_{ne} and m_{ne} are the velocity and mass of incident neutrons. (b). We now reduce Δ_b^{cry} ($= \Delta_s^{\mathrm{cry}} - \delta_{\mathrm{v}}^{\mathrm{cry}}$) to equal the superfluid bond Δ_b ($= \Delta_s - \delta_{\mathrm{v}}$) $\simeq 8.6$ °K (0.74 meV), but retain the periodic configuration. Then

$$\frac{\hbar^2 k_{\mathrm{ne}}^2}{2m_{\mathrm{ne}}} >> \Delta_s.\tag{53b}$$

Thus Δ_b can readily be excited by neutrons. Then, Eq. (52a) is no longer, in principle, an exact description for the present *inelastic* scattering. However, supplementing the condition Eq. (53b) to the conservation relations for the inelastic scattering at $q = q_b$:
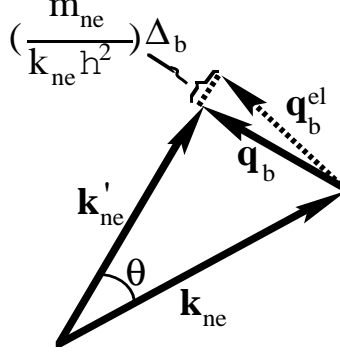
29

FIG. 9. Schematic diagram of the relationship between neutron wavevectors $k_{\neq}$ and $k'_{\neq}$ before and after an inelastic scattering, and the momentum loss q_b that is associated with the energy loss Δ_s. The Bragg condition is approximately met given that $\Delta_s << e_{\neq}$ (the incident neutron kinetic energy) and $k'_{\neq} - k_{\neq} \approx \Delta_s/\hbar e_{\neq} << k_{\neq}$, therefore $k_{\neq} \approx k'_{\neq}$. The closed vector-loop ending with $q_b{}^{el}$ represents the exact Bragg condition.

$$|\mathbf{k}'_{\mathrm{ne}} - \mathbf{k}_{\mathrm{ne}}| = q_b = \frac{2\pi}{a}, \tag{54}$$

$$\frac{\hbar^2}{2m_{\mathrm{ne}}}(k'^2_{\mathrm{ne}} - k^2_{\mathrm{ne}}) = \Delta_b, \tag{55}$$

we obtain that (55) can be adequately approximated by

$$k'_{\mathrm{ne}} \simeq k_{\mathrm{ne}}; \tag{55$'$}$$

see FIG. 9. Taken together, (54) and (55)$'$ effectively yield the Bragg condition

$$q_b \simeq 2k_{\mathrm{ne}} \sin\theta = \frac{2\pi}{a}, \tag{56}$$

which is equivalent to Eq. (52). In other words, (52a) effectively holds correct for the periodically ordered superfluid, but with $\omega = 0$ replaced by $\omega = \omega_s = \Delta_s/\hbar$. Modifying (52a) accordingly, we have

$$
\begin{aligned}
S^{\mathrm{lat}}(q)|_{\omega=\Delta_s/\hbar} &\doteq \frac{1}{N}\sum_{i,j} e^{i\mathbf{q}(\mathbf{r}_i - \mathbf{r}_j)}\delta(\omega - \Delta_s/\hbar) \\
&\doteq \int [S_b(q,\omega) + S_{\mathrm{ph}}(q,\omega)]\delta(\omega - \Delta_s/\hbar)d(\hbar\omega) \\
&= \hbar S_b^{\mathrm{lat}}(q,\omega)|_{\omega=\Delta_s/\hbar}. \qquad (q \in q_b \pm \sigma)
\end{aligned} \tag{52b}
$$

Re-ordering (52b), we get

$$
\begin{aligned}
S_b^{\mathrm{lat}}(q,\omega)|_{\omega=\Delta_s/\hbar} &= \frac{1}{\hbar} S^{\mathrm{lat}}(q)|_{\omega=\Delta_s/\hbar} \\
&= \frac{1}{N\hbar}\sum_{i,j} e^{i\mathbf{q}(\mathbf{r}_i - \mathbf{r}_j)}\delta(\omega - \Delta_s/\hbar) \qquad (q \in q_b)
\end{aligned} \tag{57}
$$

This says that $S_b^{\mathrm{lat}}(q,\omega)$ is a modified $S^{\mathrm{lat}}(q)$, and is maximal when $q = q_b$ and $\omega = \Delta_s/\hbar$. To re-emphasize, the acquisition of Eq. (52b) is a result of Δ_b being so negligibly small – of the typical energy scale of a phonon – compared to the incident neutron energy that it causes minimal departure from the Bragg condition; Δ_b is nevertheless sufficiently large to be detectable using the thermal neutrons. This incident is analogous to the thermally broadened Bragg scattering – damped by a Debye-Waller factor – in solids.

(c). We finally return from (b) to the real superfluid by disordering the atoms. A well-defined quantity is now, as with any liquid, the mean interatomic spacing a at which the radial distribution function $g(r)$ peaks. As is commonly done with regular liquids[106−108] or quasi-crystals,[109] we can replace the site summation of Eq. (57) – invovling a δ-function – with an integral involving $g(r)$ and meanwhile replace the $\delta(\omega - \Delta_s/\hbar)$ with $h(\omega - \Delta_s/\hbar)$; further combining with (50b)-(50c), we get:

$$
\begin{aligned}
S(q,\omega)|_{\omega \sim \Delta_s/\hbar} &= S_b(q,\omega)|_{\omega \sim \Delta_s/\hbar} \\
&= \frac{1}{\hbar} \, S^{\text{lat}}(q)\Big|_{\substack{\delta(r) \to g(r) \\ \delta(\omega - \Delta_s/\hbar) \to h(\omega - \frac{\Delta_s}{\hbar})}} \\
&= \frac{1}{\hbar} \left[1 + \int (g(r) - \rho) e^{i\mathbf{qr}} d\mathbf{r} \right] h(\omega - \Delta_s/\hbar), \\
&\qquad\qquad\qquad\qquad\qquad\qquad q \in q_b \pm \sigma
\end{aligned}
\tag{58}
$$

here $h(\omega - \Delta_s/\hbar) = (1/\sqrt{\pi}\sigma) \int e^{-[\hbar(\omega - \Delta_s/\hbar)/\sigma]^2} d\omega$ sharply peaks around $\Delta_s/\hbar$ and has a finite width σ. σ ought to be basically determined by the fluctuation of the atomic bond length due to the short range ordering. (58) is the scattering function due to the superfluid bond excitation. Fixing $\omega \simeq \omega_s$, we expect to see $S(q,\omega)$ to peak on the q axis; although, there is no experimental data available to us for comparison. Two further remarks can be made. First, insofar as the "Bragg" scattering is concerned, it is only meaningful to compare the $S_b(q,\omega)|_{\omega=\omega_s}$ of Eq. (58) with the zero temperature $S^{\text{cry}}(q)$ of Eq. (52a) and not with the finite temperature $S^T(q)(= \int_{-\infty}^{\infty} S^T(q,\omega)d\omega)$ of the superfluid; the $S^{\text{cry}}(q)$ of a solid at zero °K only involves the $\omega = 0$ scattering, whilst the $S^T(q)$ of the superfluid contains scatterings of all ω. Second, the correspondence between (52) and (58) not only exists in a static sense, but also in a dynamic sense, as atoms in the superfluid, viewed in $\boldsymbol{\xi}$, are localized as in a solid except that they present no long range ordering. As a basic difference from that of a normal liquid, on the other hand, the finite peak width in $g(r)$ of the superfluid is primarily due to the disordering of the atomic equilibrium positions but not atomic diffusion.

Through steps (a)-(c), the neutron scattering from the superfluid about q_b emerges to be an **inelastic damped-Bragg scattering** due to the excitation of the superfluid bond, formally described by Eq. (58).

IX. THERMODYNAMICS OF HE II

A. The partition function of the respective fluids

We consider a bulk of superfluid He II in thermal equilibrium at T, having a volume V and number of atoms N. Employing the canonical ensemble of the independent variables (T, V, N), the total partition function of the fluid formally is

$$
Z_\alpha = e^{\frac{-\Phi_0}{k_B T}} \tilde{Z}_\alpha,
\tag{59}
$$

where $\alpha = s$ for the (pure) superfluid and n for the normal fluid of He II, Φ_0 is the ground state potential energy and $e^{-\Phi_0/k_B T}$ the corresponding partition function, and $\tilde{Z}_\alpha$ is the total kinetic energy partition function. If the Z_α is known, the thermodynamic functions, the internal energy U_α, free energy A_α, entropy S_α and specific heat $C_{V\alpha}$ can then be obtained from the standard relations:

$$
U_\alpha = k_B T^2 \frac{\partial \ln Z_\alpha}{\partial T} = \Phi_0 + k_B T^2 \frac{\partial \ln \tilde{Z}_\alpha}{\partial T,}
\tag{60}
$$

$$
A_\alpha = -k_B T \ln Z_\alpha = \Phi_0 - k_B T \ln \tilde{Z}_\alpha,
\tag{61}
$$

$$S_\alpha = -\frac{\partial A_\alpha}{\partial T} = k_B \frac{\partial \left(T \ln \tilde{Z}_\alpha\right)}{\partial T} = \frac{1}{T}(U_s - A_s), \tag{62}$$

$$C_{V\alpha} = \left(\frac{\partial U_\alpha}{\partial T}\right)_{V,N}. \tag{63}$$

The microscopic theory laid out in the preceding sections enables us to treat the two fluids as independent, macroscopic systems, and the practical scheme to obtain in the following sections IX B-IX D the respective partition functions and the thermodynamic functions.

B. The pure superfluid

Consider a pure superfluid of N helium atoms, which are by Sec. II relatively localized, in the normal coordinates can be represented by N independent, identical and distinguishable (see the discussion in Sec. V Bc), effectively harmonic oscillators. With the single oscillator kinetic energy $\epsilon_n(K)$ of Eq. (23), we get the kinetic partition functions for single oscillator:

$$\begin{aligned}
z_{\mathrm{ph}}(K) &= \sum_{n=0}^{\infty} e^{\frac{\epsilon_n(\omega)}{k_B T}} = \sum_{n=0}^{\infty} e^{-(n+\frac{1}{2})\frac{\hbar\omega(K)}{k_B T}} \\
&= \frac{e^{-\hbar\omega(K)/2k_B T}}{1 - e^{-\hbar\omega(K)/k_B T}},
\end{aligned} \tag{64}$$

and for N oscillators: $\Pi_K z_{\mathrm{ph}}(K)$. Similarly the partition functions for a single and for $N_2 = \gamma N$ momentons are as Eq. (64) and $\Pi_{K_M} z_{cph}(K_M)$, with Ω in place of ω. With the above we get

$$\tilde{Z}_s = \Pi_K z_{\mathrm{ph}}(K)\Pi_{K_M} z_{\mathrm{cph}}(K_M). \tag{65}$$

Substituting Eq. (64) and its momenton counterpart in Eq. (65) and in turn, (65) in Eqs. (60)-(61), employing the identity $\ln[\Pi_K z_{\mathrm{ph}}(K)\Pi_{K_M} z_{\mathrm{cph}}(K_M)] = \sum_K \ln z_{\mathrm{ph}}(K) + \sum_{K_M} \ln z_{\mathrm{cph}}(K_M)$, we thus obtain for the (pure) superfluid:

$$\begin{aligned}
U_s &= \Phi_0 + k_B T^2 \left[\sum_K \frac{1}{z_{ph}}\frac{\partial z_{ph}}{\partial T} + \sum_{K_M} \frac{1}{z_{cph}}\frac{\partial z_{cph}}{\partial T}\right] \\
&= U_{s0} + \int_0^{\omega_D} \hbar\omega \mathcal{D}(\omega) <n(\omega)> d\omega + O_{U_M}(\Omega) \\
&\simeq U_{s0} + \frac{3Nk_B T^4}{\theta_D^3}\int_0^{y_D} \frac{y^3}{e^y - 1}dy \quad (O_{U_M} \approx 0) \\
&\simeq U_{s0} + \frac{Nk_B \pi^4 T^4}{5\theta_D^3},
\end{aligned} \tag{60a}$$

$$\begin{aligned}
A_s &= U_{s0} + k_B T \int \ln\left(1 - e^{-\hbar\omega/k_B T}\right)\mathcal{D}(\omega)d\omega + O_{AM}(\Omega) \\
&= U_{s0} + \frac{Nk_B T^4}{\theta_D^3}\int_0^{y_D} y^2 \ln(1 - e^{-y})dy \\
&= U_{s0} + \frac{Nk_B T^4}{3\theta_D^3}\left[y^3 \ln(1 - e^{-y})|_0^{y_D} - \int_0^{y_D} \frac{y^3}{e^y - 1}dy\right] \\
&\simeq U_{s0} - Nk_B \frac{\pi^4}{15}\frac{T^4}{\theta_D^3}
\end{aligned} \tag{61a}$$

32

and simply with the U_s and A_s above in the last expression of (62), we get

$$S_s \simeq Nk_B \frac{2\pi^4}{15}\left(\frac{T}{\theta_D}\right)^3 \qquad (62a)$$

here U, A and S being each in unit of J. In the above, $D(\omega) = V\omega^2/2\pi^2 c_1^3 = 3N\hbar\theta^2/k_B\theta_D^3$ (with three longitudinal modes for each K value) is the Debye density of states of N oscillators; $\theta = \frac{\hbar\omega}{k_B}$ and $\theta_D = \frac{\hbar\omega_D}{k_B} = \frac{\hbar c_1}{k_B}(\frac{6\pi^2 N}{V})^{\frac{1}{3}}$; $<n(\omega)> = \frac{1}{e^{\hbar\omega/k_B T}-1}$ is the Planck distribution. In the third expression of Eq. (60a) and the third of (61a), $y = \frac{\hbar\omega}{k_B T}$ and $y_D = \frac{\hbar\omega_D}{k_B T}$; for $y_D \to \infty$: $\int_0^{y_D} \frac{y^3}{e^y-1}dy = \sum_{p=1}^{\infty}\int_0^{\infty} y^3 e^{-py}dy = \sum_{p=1}^{\infty}\frac{6}{p^4} = \frac{\pi^4}{15}$. The momenton terms O_{U_M}, O_{A_M} and O_{S_M} are omitted in the final expressions above.

$$U_{s0} = \Phi_0 + \int \frac{1}{2}\hbar\omega\mathcal{D}(\omega)d\omega + \int \frac{1}{2}\hbar\Omega\mathcal{D}(\Omega)d\Omega + \Delta_0.$$
$$= \Phi_0 + \frac{3}{8}Nk_B(\theta_D + \gamma\Theta_D) + \Delta_0, \qquad (66)$$

is the ground-state internal energy, where Φ_0 the ground-state potential energy; $<\epsilon_n>_0 = \frac{3}{8}k_B\theta_D$, $<\epsilon_{\mathcal{N}}>_0 = \frac{3}{8}k_B\Theta_D$ and Δ_0 are the zero-point kinetic energies per atom associated with the $\mathbf{u}$, $\boldsymbol{\xi}$, and $\mathbf{R}$ motions (Sec. II). With the U_s above in (63) we get

$$C_V \simeq \frac{Nk_B 4\pi^4}{5}\left(\frac{T}{\theta_D}\right)^3 = \frac{Nk_B 2\pi^2 k_B^3 T^3}{15(N/V)\hbar^3 c_1^3}, \qquad (63a)$$

with C_V in unit of J/°K. Finally, for the superfluid in a steady flow motion of velocity $\mathbf{v}_s$, with the S_s of (62a) we obtain the entropy current

$$\mathbf{j}_S = \rho_s \mathbf{v}_s S_s = Nk_B \frac{4\pi^4 \rho_s}{15}\left(\frac{T}{\theta_D}\right)^3 \mathbf{v}_s. \qquad (67)$$

With $U_{s0} = -7.2$°K/atom and $c_1 = 239$m/sec as given previously, the above functions can be then parameterized. The resulting U_s/Nk_B, A_s/Nk_B, and S_s/Nk_B correspond to the graphs in the $T \lesssim 0.6$ °K region in FIG. 10 and these will be discussed in Sec. X. The resulting $C_V(T)$ (solid line in FIG. 3a) shows a remarkable Debye T^3 behaviour; this has been used as a fed-back information in Sec. II A. A least squares fit to the experimental data between $0 \sim 0.6$ °K using Eq. (74)′ gives $c_1 = 241$ m/sec and $\theta_D = 20$ °K. We furthermore observe that, the Debye region in the experimental C_V ends at about 0.6°K, which is in rough accordance with the usual T^3 law validity criterion,[111] $T \leq \theta_D/50 \simeq 0.4$ °K. Anomaloslly, the λ profile immediately above 0.6 (1) °K results from the second order phase transition and should not be confused with a regular ending of the T^3 region. It also is anomalous that, at T (=2.17 °K) far below θ_D (20 °K), the superfluid has already transformed to a normal liquid.

C. The normal superfluid

For the normal fluid of N identical, distinguishable and weakly interacting classical He atoms, the Boltzmann statistical mechanics expressions can be readily written down. The total partition function is

$$Z_n = e^{-\frac{U_{on}}{k_B T}}\frac{1}{N!}z^N, \qquad (68)$$

where the N factory reduces the identical distributions (due to the permutation among the N particles) to be counted as one distribution. U_{on} is similarly defined as U_{s0} of Eq. (66), and can in practice be taken as $U_{n0} = U_{s0}$, since at zero °K it reduces to the same ground

33

state as for the superfluid. $z = \sum_{i_x,i_y,i_z=0}^{\infty} e^{-E_{i_x,i_y,i_z}/k_B T}$ and $\epsilon_i = (i_x^2 + i_y^2 + i_z^2)h^2/8mV^{2/3}$ are the single atom partition function and kinetic energy.

$$z = \int_0^\infty \frac{\pi}{4}\left(\frac{8m}{h^2}\right)^{3/2} V\sqrt{E}\, e^{-E/k_B T}\, dE = \frac{V}{\Lambda^3}, \tag{69}$$

where $\Lambda = h/\sqrt{2\pi m k_B T}$ is the thermal de Broglie wavelength. Using z of (69) in Eq. (68) gives $\ln Z_n = -U_{s0}/k_B T + N\ln z - N(\ln N - e) = -U_{s0}/k_B T + N\ln(Ve/N\Lambda^3)$, where $e = 2.7183$. Placing this in equations (60)-(63) gives: $U_n = U_{s0} + \frac{3}{2}Nk_B T$ (Eq. 60b) and thus $E = \frac{3}{2}Nk_B T$, $A_n = U_{s0} + Nk_B T\ln\left[\frac{N}{Ve}\frac{h^3}{(2\pi m k_B T)^{3/2}}\right]$ (Eq. 61b), $S_n = -Nk_B \ln\left[\frac{\Lambda^3}{e^{5/2}}\frac{N}{V}\right]$ (Eq. 62b), and $C_{Vn} = \frac{3}{2}Nk_B$ (Eq. 63b).

D. The two fluid coexistent

1. Two fluid fractions.

Consider now He II is heated slowly such that at each instant the liquid can be regarded as in (quasi) equilibrium; let this start from zero Kelvin where He II is a (pure) superfluid, and $V_s(0) = V$ and $N_s(0) = N$. At a given T, by Sec. II C the fluid is a coexistent of the s regions (Sec. II): $V_s(T) = \sum_i V_{si}$, $N_s(T) = \sum_i N_i$, and the n regions: $V_n(T) = \sum_i V_{ni}$, $N_n(T) = \sum_i N_{ni}$; thus $V = V_s(T) + V_n(T)$ and $N = N_s(T) + N_n(T)$. Furthermore, by Sec. II B the s to n conversion involves the conversion of the superfluid bond Δ_b to the "van der Waals bond". The probability of the conversion is proportional to the Boltzmann factor, $1/[e^{\Delta_{sn}/k_B T} - 1] \approx e^{-\Delta_{sn}/k_B T}$, Δ_{sn} being as given in Eq. (2a). The density fractions of the two fluids of He II then follow to be

$$x_n(T) = \frac{N_n}{N} = x_{on}e^{-\frac{\Delta_{sn}}{k_B T}} = e^{-\frac{\Delta_{sn}}{k_B T}(1-T/T_o)}, \tag{70a}$$

$$x_s(T) = \frac{N_s}{N} = 1 - x_n = 1 - e^{-\frac{\Delta_{sn}}{k_B T}(1-T/T_o)} \tag{70b}$$

where $x_{n0} = e^{\frac{\Delta_{sn}}{k_B T_o}}$ is determined by satisfying the condition $x_n = 1$ at $T = T_o$, T_o being as defined in Sec. IV. x_s and x_n here and the f_s and f_n of Sec. IV, are related by: $x_s = f_s\frac{\rho_s}{\rho}$ and $x_n = f_n\frac{\rho_n}{\rho}$, and are basically equivalent since $\frac{\rho_s}{\rho} \approx \frac{\rho_n}{\rho} \approx 1$. In Eq. (2a), $E(T) = \frac{3}{2}k_B T$; and put $\delta_{vn} \approx \delta_v$, then $\Delta_b + \delta_{vn} \approx 8.6$ °K, where $\Delta_b = -7.2$ °K/atom.[88,18] Eq. (2a) is thus parameterized as:

$$\Delta_{sn} = 7.2 + 1.4 + 1.5k_B T. \tag{2a$'$}$$

As to T_o, we here only look at its limits. By the free energy function of Sec. X, the onset of $n-s$ conversion would not occur until $A_s \leq A_n$, which begins at $T \simeq 3.0$ °K (see the context of Eq. 77). On the other hand, T_o would not be lower than T_λ which is 2.17 °K from experiment. That is, $2.17 \leq T_o \leq 3.0$ °K; the evaluation of C_V in Sec. IX D 2 will show, optimally, $T_o = 2.6$ °K. With $T_o = 2.17$, 2.6 and 3.0 °K in equations (70)-(70)$'$, and with the Δ_{sn} in (2)$'$, we obtain three sets of $x_n(T,T_o)$ and $x_s(T,T_o)$ functions (solid lines in FIG. 6b). $T_o = 2.6$ °K yields indeed the optimum fractions (solid lines 3 and 3$'$ in the lower graph) which agree remarkably well with the $f_s(T)$ and $f_n(T)$ (dashed lines) obtained in Sec. IV, and are bounded by the limit fractions with $T_o = 2.17$ and 3.0 °K (solid lines 1, 1$'$ and 2, 2$'$).
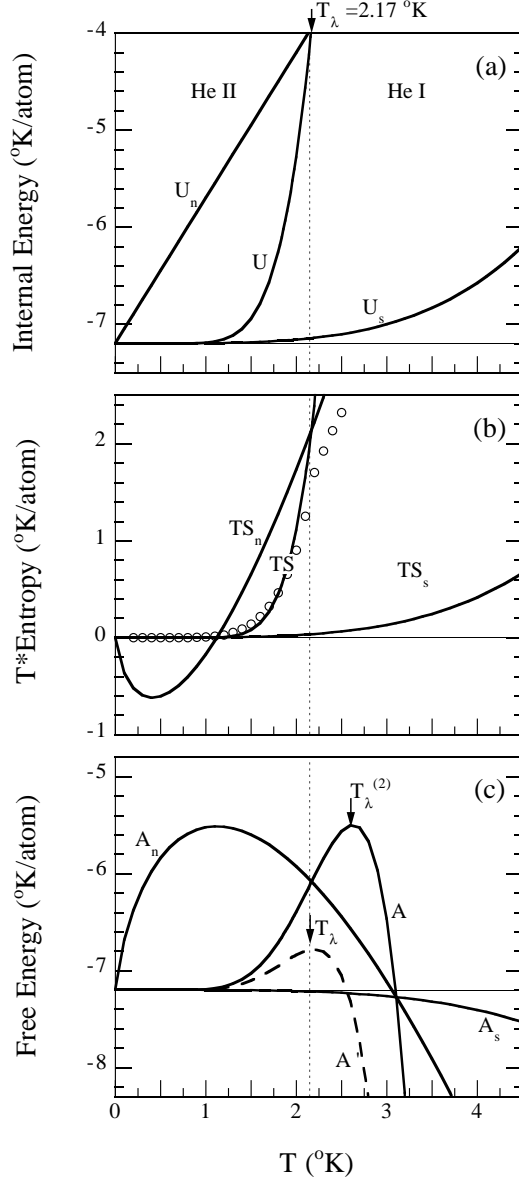
FIG. 10. Theoretical thermodynamic functions of the superfluid (s), the normal fluid (n) and their coexistent He II (without subscript) (solid lines): (a) internal energies U_s, U_n, and U as given by Eqs. (60a,b), (71)$''$, (b) entropies S_sT, S_nT, and ST as given by Eqs. (62a,b) and (73)$''$, and (c) free energies A_s, A_n, and A as given by Eqs. (61a,b) and (72)$''$. Circles in (b) represent experimental calorimetric entropy data **??**. The maximum of A of graph (c) yields the theoretical superfluid phase transition temperature $T_\lambda^{(2)}$. $T_\lambda = 2.17$ °K is the experimental phase transition temperature at SVP. For the superfluid component of He II, the functions are each given by a canonical ensemble average over the states, with a Debye type of density of states, of the independent, indistinguishable single phonons, which are produced due to in real space the harmonic oscillations in the normal coordinates of the (N) independent, localized superfluid atoms relative to $\boldsymbol{\xi}$. For the normal fluid, the functions are each a Boltzmann statistic mechanics result. The total functions result each as the weighted sum of the respective functions of the superfluid and the normal fluid, where the weighting function is given by the probability for the excitation of the superfluid bonds.

With the $x_s(T), x_n(T)$ being now known, the total thermodynamic functions of He II can be obtained as:

$$U = x_s U_s + x_n U_n, \tag{71}$$

$$A = x_s A_s + x_n A_n, \tag{72}$$

$$S = x_s S_s + x_n S_n, \tag{73}$$

$$C_V = x_s C_{Vs} + x_n C_{Vn} + \frac{\partial x_s}{\partial T}(U_s - U_n), \quad \text{and} \tag{74}$$

$$\mathbf{j}_{Entr} = \rho_s \mathbf{v}_s S_s / N k_B + \rho_n \mathbf{v}_n S_n / N k_B. \tag{75}$$

.1. Between 0 to 0.6 °K. Here equations (70) give $x_s(T) \simeq 1$ and $x_n(T) \simeq 0$, as we have already assumed so when representing the He II in this T region with Eqs. (60a)-(62a) and (67); compare FIG. 6b. Hence Eqs. (71)-(75) reduce to Eqs. (60a)-(62a) and (67).

.2. Between 0.6 ($\sim$ 1) to 2.17 °K (T_λ). Here a drastic conversion from the superfluid to the normal fluid occurs, with both of the fluids in Eqs. (71)-(75) having significant weights: $0 < x_s, x_n < 1$. By Sec. II C the two fluids of He II here aggregate in macroscopically large separate regions, thus the lattice statistical thermodynamics results (Sec. IX B) – strictly each plus a higher order term $O_Y(T)$ (YU_s, A_s, or S_s), and the Boltzmann statistics results (Sec. IX C) apply to each fluid regions, across the entire transition T regime except in the immediate proximity of the critical point T_λ where the atomic dynamics of both the fluids become strongly long-range cooperative, for which our present treatment would not hold valid. Using in Eqs. (71)-(74) the thermodynamic functions of Eqs. (60a)-(62a) and (67) for the superfluid terms, of (60b)-(62b) for the normal fluid terms, and the x_s and x_n of Eqs. (71)-(71)′, we obtain:

$$U = U_{s0} - (U_{s0} - U_{on}) e^{-\frac{\Delta_{sn}}{k_B T}(1 - \frac{T}{T_o})} + N k_B \left\{ \frac{\pi^4 T^4}{5\theta_D^3} - \left[\frac{\pi^4 T^4}{5\theta_D^3} - \frac{3}{2} k_B T \right] e^{-\frac{\Delta_{sn}}{k_B T}(1 - \frac{T}{T_o})} + O_U(T) \right\}, \tag{71''}$$

$$A = U_{s0} - (U_{s0} - U_{on}) e^{-\frac{\Delta_{sn}}{k_B T}(1 - \frac{T}{T_o})} + N k_B \left\{ -\frac{\pi^4}{15} \frac{T^4}{\theta_D^3} + \left[\frac{\pi^4}{15} \frac{T^4}{\theta_D^3} + T \ln \left(\frac{N}{Ve} \frac{h^3}{(2\pi m k_B T)^{3/2}} \right) \right] \right.$$

$$\left. e^{-\frac{\Delta_{sn}}{k_B T}(1 - \frac{T}{T_o})} + O_A(T) \right\}, \tag{72''}$$

$$S = N k_B \left\{ \frac{4\pi^4}{15} \left(\frac{T}{\theta_B} \right)^3 - \left[\frac{4\pi^4}{15} \left(\frac{T}{\theta_B} \right)^3 + \ln \left(\frac{\Lambda^3}{e^{5/2}} \frac{N}{V} \right) \right] e^{-\frac{\Delta_{sn}}{k_B T}(1 - \frac{T}{T_o})} + O_S(T) \right\}, \tag{73''}$$

$$C_V = N k_B \left\{ \frac{4\pi^4}{5} \left(\frac{T}{\theta_D} \right)^3 + \left[\frac{3}{2} \left(1 + \frac{\Delta_{sn}}{k_B T} \right) - \frac{4\pi^4}{5} \left(\frac{T}{\theta_D} \right)^3 \left(1 - \frac{\Delta_{sn}}{4 k_B T} \right) \right] e^{-\frac{\Delta_{sn}}{k_B T}(1 - \frac{T}{T_o})} \right\}. \tag{74''}$$

We first evaluate C_V. Using in Eq. (74)″ the two limiting values 2.17 and 3 °K for T_0 as discussed in the beginning of this section and Δ_{sn} of Eq. (2b), we obtain two $C_V(T)$ limits (solid lines -1 and -2 in FIG. 3b), which fall near to, actually enclosing in the middle, the experimental λ-profile (circles), therefore defining a region of uncertainty in the theoretical $C_V(T)$. Within the limits, we find at $T_o = 2.6$ °K the $C_V(T)$ (solid line -3) optimally matches the experimental C_V data (circles). The remarkably good prediction of C_V and similarly x_s (x_n) earlier both with $T_o = 2.6$ °K, although being fortuitous in principle, can however find the following physical explanation. First, an effective T_o intermediate between

2.17 and 3.1 °K is expected to exist as discussed earlier. Second, it can be shown that the λ-profile is primarily sensitive to the exponent, in which, the only other parameter Δ_s, thus Δ_{sn}, is given consistently by various experiments (cf. Sec. II).

The first order functions, Eqs $(71)''$-o$(73)''$ for the coexistent, Eqs. (60a)-(62a) for the pure superfluid and Eqs. (60b)-(62b) for normal fluid, can be parameterized, with the values for θ_D, Δ_s, and T_0 (2.6 °K) as above and $U_{0s} = -7.2$ °K/atom as used several times earlier. The resulting functions are graphically shown in FIG. 10, a, b, c, across the whole T range of He II; for the entropy there exist experimental data (circles in FIG. 10b),[84−86] with which the theoretical function $S(T)$ agrees satisfactorily, except for a noticeable suppression about the T_Λ as can be expected. We observe several as-expected features for $T < T_\lambda$: 1). The internal energy and hence the kinetic energy $< \epsilon_n >= (U_s - U_{s0})/Nk_B$, the entropy (at the high T end) and the free energy of the pure superfluid are qualitatively lowered compared to those of the normal fluid, by $< \epsilon_n > -E_{nr} = -(U_s - U_n)/Nk_B \sim 3.1$, $(S_s - S_n)/Nk_B \sim 2$, and $(A_s - A_n)/Nk_B = 1$ °K/atom respectively at T just below 2.17 °K. 2) From about 0.6 °K the total functions (of the coexistent) asymptotically approach to the corresponding functions of the pure superfluid with falling T, simultaneously He II approaches to a predominately pure superfluid: $x_s \to 1$. 3). The entropy of the normal fluid from 2.17 K reduces rapidly with falling T from T_λ, and to a negative function in the regime below ~ 0.6 °K, in which it becomes the significant source of the large positive A_n, or, of the normal fluid phase instability. Instead, the localized coherent oscillation scheme of the superfluid produces here a relatively high degree of disorder. 4). $U_s \simeq U_{s0}$ on the scale of U_{s0}. 5). With $\theta_D = 20$ °K obtained above, we have the zero-point vibrational energy per atom of the **u**- motion (see the discussion below Eq. 66):

$$< \epsilon_n >_0 /Nk_B = 7.5 \quad (^oK/\text{atom}) \tag{76}$$

X. THE SUPERFLUID PHASE TRANSITION AND T_λ

Near T_λ, from FIG. 10 we observe that the first order functions of each pure fluid component all suffer discontinuous changes on transforming from one (normal) component to the other (superfluid). However, as the phase transition involves a gradual conversion from one (the normal) component to the other (the superfluid), from $x_n(T_o) = 1$ to $x_n(0) = 0$, the first-order total thermodynamic functions of the coexistent, He II, are continuous; this is as expected for the second order phase transition here.

Futhermore, from FIG. 10 the onset of the n-s conversion can clearly be seen to occur near to 3.0 °K, where a lower A_n switches to a lower A_s:

$$A_s(T_\lambda) - A_n(T_\lambda) \leq 0. \tag{77}$$

With the A_s and A_n given in (61a) and (61b), (77) becomes

$$e^{-19.2(T/\theta_D)^3} \leq \frac{nh^3}{e\sqrt{2\pi mk_BT}^3}. \tag{77$'$}$$

Since $19.2(T/\theta_D)^3 << 1$ for the He II temperatures, we can write the left hand side of $(77)'$ as $e^{-19.2(T/\theta_D)^3} \approx 1$ and re-ordering, we obtain

$$T_\lambda^{(1)} \simeq \left(\frac{N}{Ve}\right)^{2/3} \frac{h^2}{2\pi mk_B}. \tag{78}$$

It is noteworthy that this $T_\lambda^{(1)}$, as a direct statistical thermodynamic result for the two fluids of He II, is basically identical to the T_λ given by London,[18,34] although London's T_λ was obtained, whilst lacking a direct thermodynamic scheme, by imposing a limitation in the thermal wavelength obtained for the normal fluid based on Boltzmann statistical mechanics.

Placing now in Eq. (78) the experimental critical density of He II, $n = \frac{N}{V} = 2.182 \times 10^{28}$ atoms/m^3, and the values for the other constants as previously specified, we obtain

$$T_\lambda^{(1)} \simeq 3.05 \quad {}^oK. \tag{78$'$}$$

However, theoretically the initial n-s conversion under the condition (77), onsetting at $T_\lambda^{(1)}$, does not lead the total free energy A to maximum until $T^{(2)}$, as can be seen in FIG. 10c (solid curve). It is the A maximum which resembles the critical instability of the system in the second order phase transition, and where a qualitative $n - s$ conversion will occur. This critical condition formally writes:

$$\frac{\partial^2 A}{\partial T^2} = 0, \tag{79}$$

which expands as

$$\frac{\Delta_{sn}}{k_B T^2}\left(\frac{\Delta_{sn}}{k_B T^2} - \frac{2}{T}\right)(A_n - A_s) + \frac{2\Delta_{sn}}{k_B T^2}\frac{\partial}{\partial T}(A_n - A_s)$$
$$+ \frac{\partial^2}{\partial T^2}(A_n - A_s) = 0. \tag{79$'$}$$

Here the first order term of $(A_n - A_s)$ represents just the condition (77), and the first and second derivative terms of $(A_n - A_s)$ are additional; (79)$'$ is a complex second order differential equation of $A_n - A_s$. Now instead of seeking an analytical solution of Eq. (79), we can readily graphically locate, as we just actually did, the critical temperature from the A maximum in FIG. 10c to be:

$$T_\lambda^{(2)} \simeq 2.6 \qquad {}^oK. \tag{80}$$

Compared to $T_\lambda^{(1)}$, $T_\lambda^{(2)}$ is seen to be lowered in value in closer agreement with the experimental value 2.17 °K, although with still a quite large discrepancy. The major error source may be the neglect of a strong atomic correlation which anticipates to present already in the normal fluid in this T range, in presumably a similar way as in its destination state – the superfluid; indeed previous studies[24] have actually shown that the normal liquid He I deviates from ideal gas when nearing T_λ. Correlation will suppress the A_n value, thereby yield a lowered value for $T_\lambda^{(2)}$. If assuming across the transition T region A_n is uniformly modified to A_n' and hence A to A' and letting the maximum of A' yield the experimentally observed T_λ, we find $A_n' \approx A_n - 0.7$ °K and $A' = A - 0.7$ °K (dashed curve in FIG. 10).

APPENDIX A: DISTINCTION OF CONDITIONS FOR "FLUIDITY" AND "DIFFUSIVITY".

The preceding discussions in effect imply that with the superfluid He II fluidity is not accompanied by any discernible atomic diffusion. In combination with the equations of motions and their solution in Secs. V B and V C, and, based on the well-understood characteristics of the liquid and solid systems, we now elucidate that these two kinds of phenomena do not need co-occur. Fluidity is a phenomenon that any part of the fluid can move relative to another, in a flexible manner and under a small degree of shear stress. In respect of motion, the realization of a "flow" only requires the collective translation of all of the atoms concerned; there is nothing specific about whether the individual atoms diffuse in the same time. In respect of the atomic interaction, fluidity results from the absence of shear elasticity, or, the condition that the shear attraction between the atoms is so weak such that the system is unable to resist any shearing pressure. This character, in the matrix form of the interatomic force $\mathbf{F}$ below, is represented by that the shear (tangential) attraction force terms – the off diagonal components – are zero (cf. also Eq. (22)):

$$\mathbf{F} = \begin{pmatrix} F_{xx}{}^r + F_{xx}{}^a+ & 0 & 0 \\ 0 & F_{yy}{}^r + F_{yy}{}^a & 0 \\ 0 & 0 & F_{zz}{}^r + F_{zz}{}^a \end{pmatrix}$$
$$(\text{ liquid at rest}); \tag{A1}$$

or,

$$\mathbf{F} = \begin{pmatrix} F_{xx}{}^r + F_{xx}{}^a & F_{xy}{}^r & F_{xz}{}^r \\ F_{yx}{}^r & F_{yy}{}^r + F_{yy}{}^a & F_{yz}{}^r \\ F_{zx}{}^r & F_{zy}{}^r & F_{zz}{}^r + F_{zz}{}^a \end{pmatrix},$$
$$(\text{liquid in flow motion.}) \tag{A2}$$

For the liquid at rest as of (A1), all the off-diagonal force terms are zero, and the diagonal components $F_x = F_y = F_z$ consist of the tensile attraction force ($F_{\alpha\alpha}^a$) and repulsion force ($F_{\alpha\alpha}^r$), where $\alpha = x, y, z$; the equality of the diagonal terms represents the isotropy of the liquid. When in flow motion as of (A2), the shear repulsion force terms, i.e. the off-diagonals, are finite and this leads to viscosity. On the other hand, as of Eq. (A1) or (A2), for the liquid either at rest or in flow motion, the tensile attraction force terms are finite and this represents that the atoms are attracted to each other (true for all liquids). The above are to be contrasted to the force condition for an elastic solid:

$$\mathbf{F} = \begin{pmatrix} F_{xx}{}^r + F_{xx}{}^a & F_{xy}{}^r + F_{xy}{}^a & F_{xz}{}^r + F_{xz}{}^a \\ F_{yx}{}^r + F_{yx}{}a & F_{yy}{}^r + F_{yy}{}^a & F_{yz}{}^r + F^a{}_{yz} \\ F_{zx}{}^r + F_{zx}{}^a & F_{zy}{}^r + F_{zy}{}^a & F_{zz}{}^r + F_{zz}{}^a \end{pmatrix}$$
$$(\text{elastic body}). \tag{A3}$$

where, the diagonal terms are generally not zero, whence yielding the rigidity. Diffusion, on the other hand, is produced if the gradients of some of the tensile force terms – the diagonal terms – are finite; e.g. diffusion in x direction results from $\partial F_{xx}/\partial x \neq 0$ which leads to a density flux $D\partial F_{xx}/\partial x$; cf. Eq. (13.b). The tensile force terms exist for both solid and liquid, this feature corresponding to the characteristically finite values of the diagonals in all the above matrices. Hence diffusion can identically occur in both the systems; or, they may identically not occur if the kinetic energy of the atoms is low, roughly lower than the (tensile) attraction potential barrier between adjacent atoms. It is true that, in regular fluids, a trivial shearing elasticity is often accompanied by a high mobility of the single atoms. This is nevertheless not so in the superfluid, where the many quantum atom correlation (Sec. III) produces a contrast in the tensile and shearing interactions, and the significantly large tensile attraction prevents the atoms from diffusion.

[1] W H Keesom, *Helium*, (Elsevier Publishing Comp, Amsterdam, 1942)

[2] W. H. Keesom and J. N. van der Ende, Proc. Roy. Acad. Amsterdam **33**, 243 (1930).

[3] J. F. Allen and A. D. Misener, Nature **141**, 75 (1938); Proc. Roy. Soc. London **A172**, 467 (1939).

[4] P. Kapitza, Nature **141**, 74 (1938).

[5] J. D. Reppy and D. Depatie, Phys. Rev. Lett. **12**, 187 (1964).

[6] J. B. Mehl and W. Zimmerman, Jr, Phys. Rev. Lett. **14**, 815 (1965); Phys. Rev. **167**, 214 (1968).

[7] R. P. Henkel, G. Kukich and J. D. Reppy, in Proceedings of the eleventh International Conference on Low Temp Phys, St Andrews, Scotland, Editor J F Allen, D M Finlayson and D M McCall (Univ. of St Andrews Press, St Andrews, Scotland, 1968) p 178; Bull. Am. Phys. Soc. **13**, 663 (1968).

[8] J. F. Allen and J. Jones, Nature **141**, 243 (1938).

[9] F. Simon, Nature **133**, 460, 529 (1934).

[10] H. Kamerlingh Onnes, Proc. Roy. Acad. Amsterdam **13**, 1903 (1911).

[11] W. F. Vinen, Nature **181**, 1524-25 (1858); Proc. Roy. Soc. **A260**, 218 (1961).

[12] G. W. Rayfield and F. Reif, Phys. Rev. **136**, A1194 (1964).

[13] S. C. Whitmore and W. Zimmermann, Phys. Rev. **166**, 181-96 (1968).

[14] W. H. Keesom and K. Clusius, Proc. Roy. Acad. Amsterdam **35**, 307 (1932); Leiden Commun **219c**; W H Keesom and A P Keesom, Proc. Roy. Acad. Amsterdam **35**, 736 (1932).

[15] H. Palevsky, K. Otnes and K. E. Larsson, Phys. Rev. **112**, 11 (1958); H. Palevsky, et al., ibid., **108**, 1346-7 (1957).

[16] J. F. Allen, R. Peierls, and M. Zaki Uddin, *Narure* **140**, 62 (1937).

[17] F. E. Simon and C. A. Swenson, Nature **165**, 829 (1950); C. A. Swenson, Phys. Rev. **79**, 626 (1950); **86**, 870 (1952); **89**, 538 (1953); J. S. Dugdale and F. E. Simon, Proc. Rpy. Soc. London **A218**, 291 (1953).

[18] F. London, *Superfluids, Vol II, Macroscopic Theory of Superfluid Helium*, (John Wiley & Sons, Inc., New York, London, 1954).

[19] C. J. Gorter, editor, *Progress in low temperature physics*, Vols. I-VI, (Interscience Publisher, New York, 1955-1970).

[20] K. R. Atkins, *Liquid Helium*, (Cambridge Univ. Press, 1959).

[21] I. M. Khalatnikov, *An Introduction to the Theory of Superfluidity*, (W. A. Benjamin Inc., New York, Amsterdanm, 1965).

[22] P. A. Egelstaff, *An introduction to the Liquid State*, (Academic Press, London and New York, 1967), Chapter 16.

[23] W. E. Keller, *Helium-3 and Helium-4*, (Plenum, New York, 1969).

[24] J. Wilks, *The Properties of Liquid and Solid Helium*, (Clarendon Press, Oxford, 1967); *An Introduction to Liquid Helium*, Clarendon Press, Oxford (1970); J. Wilks and D. S. Betts, *An Introduction to Liquid Helium*, (Clarendon Press, Oxford, 1987) 2nd edition.

[25] A. D. B. Woods and R. A. Cowley, Rep. Prog. Phys. **36**, 1135 (1973).

[26] K. H. Bennemann, and J. B. Ketterson, editors, *The physics of liquid and solid helium*, Parts I & II, (John Wiley & Sons, New York, 1975).

[27] D. E. Brewer, editor, *Progress in Low Temperature Physics*, Vol. VII (1978) to Vol XIII (1992);

[28] D. R. Tilley and J. Tilley, *Super fluidity and Super conductivity*, 2nd edition, (Adam Hilger Ltd, Bristol and Boston, 1986), pp. 8.

[29] H. R. Glyde and E. C. Svensson, "Solid and Liquid Helium", in *Methods of Experimental Physics*, p. 303-403 (Academic Press, Inc. and Atomic Energy of Canada Limited, 1987).

[30] P. Nozieres and D. Pines, *The Thoery of Quantum Liquids* Vol. 2, (Addison-Wesley Publishing Co. Inc., 1990).

[31] R. J. Donnelly, *Quantized vortices in helium II*, (Cambridge Univ. Press, 1991), Editors: A. M. Goldman, P. V. E. McClintock, M. Springford.

[32] P V E McClintock, J K Wigmore, *Low-Temperature Physics: an introduction for scientists and engineers* (Blackie, Glasgow and London, 1992).

[33] A. Griffin, *Excitations in a Bose-Condensed Liquid*, (Cambridge Univ. Press, Cambridge, 1993).

[34] F. London, Nature (London) **141**, 643 (1938).

[35] L. Landau, J. Phys. (USSR) **5**, 71 (1941); **11**, 91 (1947).

[36] R. P. Feynman, Phys. Rev. **91**, 1291; 1301 (1953); Phys. Rev. **94**, 262 (1954); Prog. Low. Temp. Phys., edited by Gorter (North Holland, 1955).

[37] Tisza, Nature **141**, 913 (1938).

[38] N. Bogoliubov, J. Phys. **XI**, 23 (1947).

[39] M. Cohen and R. P. Feynman, Phys. Rev. **107**, 13 (1957); R. P. Feynman and M. Cohen, Phys. Rev. **102**, 1189 (1956).

[40] D. Pines, in *Quantum Fluids: proceedings of the Sussex University Symposium*, Edited by D F Brewer (North-Holland, Amsterdam, 1966).

[41] T. D. Lee and K. Huang and C. N. Yang, Phys. Rev. **106**, 1135 (1957).

[42] H. R. Glyde and A. Griffin, Phys. Rev. Lett. **65**, 1454 (1990).

[43] P. Debye, Ann. Phys. **39**, 789 (1912).

[44] A concise, clear summary is given e.g. in the review of Ref. 25.

[45] P. A. Whitlock and R. M. Panoff, Can. J. Phys. **65**, 1409 (1987).

[46] A. Griffin, D. W. Snoke, S. Stringarei, edit, *Bose Einstein Condesation*, (Cambridge University Press, 1995).

[47] W. L. McMillan, Phys. Rev. **A 138**, 442 (1965)

[48] R. Jastrow, Phys Rev **98** 1479 (1955).

[49] S. A. Vitiello, K. Runge, G. V. Chester, and M. H. Kalos, Phys. Rev. B **42**, 228 (1990).

[50] T. McFarland, S. A. Vitiello, L. Reatto, G. V. Chester, and M. H. Kalos, Phys. Rev. **50**, 13577 (1994-II); and Res. therein.

[51] D. M. Ceperley, Rev. Mod. Phys. **67** , 279-355 (1995); and refs. therein.

[52] R. P. Feynman and A. R. Hibbs, *Quantum Mechanics and Path Integrals*, (McGraw-Hill, New York, 1965).

[53] M. Boninsegni, D. M. Ceperley, J. Low Temp. Phys. **104**, 339-57 (1996).

[54] C. W. Woo, in: *The physics of liquid and solid helium*, edited by K. H. Bennemann and J. B. Ketterson, Parts I, (John Wiley & Sons, New York, 1975), p. 349.

[55] J. X. Zheng-Johansson, B. Johansson and P-I. Johansson, "The superfluidity mechanism of He II", submitted to Phys. Rev. (2000); http://arXiv.org/abs/cond-mat/0206339.

[56] J. X. Zheng-Johansson, et al., private communications with a few specialists in the field (2000, 2001).

[57] J. X. Zheng-Johansson and B. Johansson, in *Dynamics in Confinement*, edited by B. Frick, R. Zorn and H. Büttner, J. de Physique IV **10**, Pr7-181 (2000). J. X. Zheng-Johansson, XXII Int. Conf. Low Temp. Phys. Abstracts, pp. 296 (Helsinki, 1999.a); Bulletin of the Amer. Phys. Soc. – Centennial Meeting **44**, 193 (1999.b); Internal report: *The Theory of Superfluidity of ^4Helium*, (The Zheng-Johansson Publishing, Nyköping, Sweden, Nov. 15, 1998); Cond-mat/9901125.

[58] D G Hurst and D G Henshaw, Phys. Rev. **100**, 994-1002 (1955)

[59] D. G. Henshaw, Phys. Rev. **119** 9-13 and 14-21 (1960).

[60] E. K. Achter and L. Meyer, Phys. Rev. **188** 291-300 (1969).

[61] R. B. Hallock, Phys. Rev. A**5**, 320-30 (1972).

[62] W. I. Gordon, C. H. Shaw and J. G. Daunt, J. Phys. Chem. Solids **5**, 117-128 (1958).

[63] W. H. Keesom and K. W. Taconis, Physica **4**, 28, 256 (1937); **5**, 270 (1938).

[64] E. L. Andronikashvili, Zh eksp theo Fiz **16**, 780 (1946).

[65] V. P. Peshkov, Dokl. Akad. Nauk SSSR **45**, 365 (1944); J. Phys. Moscow **8**, 381 (1944); **10**, 389 (1946); Proc. Conf. Low Temp. Phys. (Physical Society, London, 1947), pp.19.

[66] W.Y. Tam and G. Ahlers, J. Low Temp. Phys. **66**, 173 (1987)

[67] D. G. Henshaw and A. D. B. Woods, Phys. Rev. **121**, 1266 (1961).

[68] A. D. B. Woods, E. C. Svensson, Phys. Rev. Lett. **41** 974, (1978); E. C. Svensson, R. Scherm and A. D. B. Woods, in Proc. of the Fifteenth Int. Conf. on Low Temp. Phys. (Grenoble-France, 1978).

[69] E. C. Svensson, in: *Elementary Excitations in Quantum Fluids*, pp.59, K. O. Ohbayashi, M. Watabe, editors, Proceedings of the Hiroshima Symposium, Hiroshima, Japan, August 17-18, 1987 (Springer-Verlag, 1989).

[70] W. G. Stirling and H. R. Glyde, Phys. Rev. **B41**, 4224 (1990).

[71] O. Plantevin, B. Fåk, H. R. Glyde, N. Mulders, J. Bossy, G. Coddens and H. Schober, Phys. Rev. **B63**, 224508 (2001).

[72] O. Plantevin, B. Fåk, and H. R. Glyde, J. de Physiq. IV **10**, 177 (2000).

[73] B. Fåk, O. Plantevin, H. R. Glyde, and N. Mulder, Phys. Rev. Lett. **85**, 3886 (2000); H. R. Glyde, O. Plantevin, B. Fåk, G. Coddens, P. S. Danielson and H. Schober, ibid., **84**, 2646 (2000).

[74] Excitation properties of He II at higher q values than 1.93 1/Å have been studied in detail by various authors, see e.g. W. M. Snow and P.E. Sokol, J. Low Temp. Phys **101**, 881 (1995); T. R. Sosonick, W. M. Snow, R. N. Silver and P. E. Sokol, Phys. Rev. B **43**, 216 (1991) and Refs. therin; B. Fåk and K. H. Andersen, Physics Letters A **160**, 468 (1991) and Refs. therein. This

q region involves primarily the translational kinematics of the helium nuclei; this is not covered in the discussions of the present paper.

[75] E. C. Sevnsson, Private communication (1999).

[76] K. R. Atkins and R. A. Stasior, Can. J. Phys. **31**, 1156 (1953).

[77] K. Sköld and K. E. Larsson, Phys. Rev. **161**, 102 (1967).

[78] P. A. Egelstaff, Rep. Prog. Phys. **29** 333, (1966).

[79] J. R. D. Copley and J. M. Rowe, Phys. Rev. Lett. **32**, 49 (1974).

[80] J. R. D. Copley and S. W. Lovesey, Rep. Prog. Phys. **38**, 461-563 (1975).

[81] A. D. B. Woods, Phys. Rev. Lett. **14**, 355 (1965).

[82] P. C. Hohenberg, P. C. Martin, Phys. Rev. Lett. **12**, 69 (1964).

[83] As simple cubic, or any other crystal structure, is not an exact representation of the actually disordered superfluid, hence the $a = 3.3$ is only close but not equal to the lattice constant $a_\rho = 3.6$ which one would obtain if assuming a simple cubic structure with the experimental density of He II, $\rho = 0.146$ g/cm^3 as input.

[84] J. Wiebes, C. G. Niels-Hakkenberg and H. C. Kramers, Physica **23**, 625 (1957).

[85] J. D. Wasscher and C. J. Gorter, Physica **18**, 329 (1952).

[86] R. W. Hill and O. V. Lounasmaa, Phil. Mag. **2**, 143 (1957).

[87] D. Greywall, Phys. Rev. B **18**, 2127 (1978); **21** 1329 (1979) (Erratum).

[88] F. E. Simon and C. A. Swenson, Nature **165**, 829 (1950); C. A. Swenson, Phys. Rev. **79**, 626 (1950).

[89] E. F. Talbot and H. R. Glyde and W. G. Stirling and E. C. Svensson, Phys. Rev. B **38**, 11229 (1988).

[90] E. C. Svensson, W. Montfrooij and I. M. de Schepper, Phys. Rev. Lett. **77**, 4398 (1996).

[91] J. L. Yarnell, G. P. Arnold, P. J. Bendt and E. C. Kerr, Phys. Rev. **113**, 1379 (1959); P. J. Bendt, R. D. Cowan and J. L. Yarnell, ibid., **113**, 1387 (1959).

[92] R. J. Donnelly, J. A. Donnelly and R. N. Hills, J. of Low Temp. Phys. **44**, 471 (1981).

[93] G. Careri, F. Scaramuzzi and J. O. Thomoson, Nuovo Cim. **13**, 186 (1959).

[94] F. Reif and L. Meyer, Phys. Rev. **119**, 1164 (1960); L. Meyer and F. Reif, Phys. Rev. **123** 727 (1961).

[95] T. Ellis, P. V. E. McClintock, Phil. Trans. Roy. Soc. **A315**, 259 (1985).

[96] K. R. Atkins and D. V. Osborne, Phil. Mag. **41** 1078 (1950).

[97] F. London, Z. Phys. Chem. (B) **11** 222 (1930); Trans. Far. Soc. **33**, 8 (1937).

[98] F. Seitz, *The modern theory of solids*, (McGraw Hill, New York, London, 1940).

[99] E. C. Kerr and R. D. Taylor, Ann. Phys. **26**, 292 (1964).

[100] D. G. Henshaw and A.D.B. Woods, Proc. 7th Int. Conf. Low Temp. Phys. editors Graham and Hollis Hallett page 539 (North Horland, 1961).

[101] e.g. E. Merzbacher, *Quantum Mechanics* 2nd edition, (John Wiley & Sons, New York, 1970), p. 107

[102] See e.g. N W Ashcroft and N D Mermin, *Solid State Physics*, (Saunders College, Philadelphia, 1976), pp. 506-8.

[103] H. Lamb, *Hydrodynamics*, 6th edition, (Cambridge University Press, New York, 1932).

[104] H. A. Fairbank and J. Wilks, Proc. Roy. Soc. **A 231**, 545 (1955).

[105] Cohen and Feynman's evaluation of phonon-phonon collision time, Phys. Rev. **107**, 13 (1957), and also that given by Landau and Khalatniko (1949), which corresponds to a peak width in the dynamic structure factor $< 10^{-6}$ °K, should in principle apply to the present phonons, as it is chiefly the atomic dynamics scheme for producing the phonons that differs in the present theory from Landau and Feynman's theory.

[106] P. A. Egelstaff, *An introduction to the liquid state*, (Academic Press, New York, 1967).

[107] G. E. Bacon, *Neutron Diffraction* 3rd edition, (Clarendon Press, Oxford, 1975).

[108] G. L. Squires, *Introduction to the theory of thermal neutron scattering*, (Cambridge Univ. Press, Cambridge, 1978).

[109] C. Janot, *Quasicrystals, A Primer*, second edition, (Oxford Science Publications, Oxford, 1994).

[110] The fact that the experimentally observed well defined excitation energy $\omega(K)$ makes a compelling evidence that the distortion here cannot have been caused by the fluctuation in cage parameters as we unrealistically proposed earlier.

[111] C. Kittel, *Introduction to Solid State Physics*, 6th edition, (John Wiley & Sons, Inc., New York, 1986).